Petra Éva Szili

Deciphering resistance against multi-targeting antibiotics

Supervisor: Csaba Pál, D.Sc.

Synthetic and Systems Biology Unit

Biological Research Centre

Szeged

Multidisciplinary Medical Sciences Doctoral School

University of Szeged

Albert Szent-Györgyi Medical School

Institute of Biochemistry

Szeged

2023

Table of Contents

List of Publications

Number of peer-reviewed scientific publications: 10 (1 first-author, 9 co-authored)

Number of citations (independent citations): 125 (77)

H-index: 4

Total impact factor: 43.4

Publications that served as a basis for the dissertation:

I. Ákos Nyerges, Bálint Csörgő, Gábor Draskovits, Bálint Kintses, Petra Szili, Györgyi Ferenc, Tamás Révész, Eszter Ari, István Nagy, Balázs Bálint, Bálint Márk Vásárhelyi, Péter Bihari, Mónika Számel, Dávid Balogh, Henrietta Papp, Dorottya Kalapis, Balázs Papp, and Csaba Pál (2018). Directed evolution of multiple genomic loci allows the prediction of antibiotic resistance. Proceedings of the National Academy of Sciences, 115(25), E5726-E5735.
Impact factor: 9.58, SJR indicator: D1 (Multidisciplinary)

II. Petra Szili, Gábor Draskovits, Tamás Révész, Ferenc Bogár, Dávid Balogh, Tamás Martinek, Lejla Daruka, Réka Spohn, Bálint Márk Vásárhelyi, Márton Czikkely, Bálint Kintses, Gábor Grézal, Györgyi Ferenc, Csaba Pál, Ákos Nyerges (2019). Rapid evolution of reduced susceptibility against a balanced dual-targeting antibiotic through stepping-stone mutations. Antimicrobial agents and chemotherapy, 63(9), e00207-19.
Impact factor: 4.904, SJR indicator: D1 (Infectious Diseases)

III. Akos Nyerges, Tihomir Tomašič, Martina Durcik, Tamas Revesz, Petra Szili, Gabor Draskovits, Ferenc Bogar, Žiga Skok, Nace Zidar, Janez Ilaš, Anamarija Zega, Danijel Kikelj, Lejla Daruka, Balint Kintses, Balint Vasarhelyi, Imre Foldesi, Diána Kata, Martin Welin, Raymond Kimbung, Dorota Focht, Lucija Peterlin Mašič, Csaba Pal (2020). Rational design of balanced dual-targeting antibiotics with limited resistance. PLoS biology, 18(10), e3000819.
Impact factor: 8.029, SJR indicator: D1 (Biochemistry, Genetics and Molecular Biology)

Combined impact factor: 22,513

Other related publications:

IV. Andraž Lamut, Žiga Skok, Michaela Barančoková, Lucas J Gutierrez, Cristina D Cruz, Päivi Tammela, Gábor Draskovits, Petra Éva Szili, Ákos Nyerges, Csaba Pál, Peter Molek, Tomaž Bratkovič, Janez Ilaš, Nace Zidar, Anamarija Zega, Ricardo D Enriz, Danijel Kikelj, Tihomir Tomašič (2020). Second-generation 4, 5, 6, 7-tetrahydrobenzo

[d] thiazoles as novel DNA gyrase inhibitors. Future Medicinal Chemistry, 12(04), 277-297.
Impact factor: 3.808 , SJR indicator: Q2 (Drug Discovery)

V. Benedetta Fois, Žiga Skok, Tihomir Tomašič, Janez Ilaš, Nace Zidar, Anamarija Zega, Lucija Peterlin Mašič, Petra Szili, Gábor Draskovits, Ákos Nyerges, Csaba Pál, Danijel Kikelj (2020). Dual Escherichia coli DNA Gyrase A and B Inhibitors with Antibacterial Activity. ChemMedChem, 15(3), 265-269.
Impact factor: 3.466, SJR indicator: Q1 (Pharmacology, Toxicology and Pharmaceutics)

VI. Martina Durcik, Žiga Skok, Janez Ilaš, Nace Zidar, Anamarija Zega, Petra Éva Szili, Gábor Draskovits, Tamás Révész, Danijel Kikelj, Akos Nyerges, Csaba Pál, Lucija Peterlin Mašič, Tihomir Tomašič (2021). Hybrid Inhibitors of DNA Gyrase A and B: Design, Synthesis and Evaluation. Pharmaceutics, 13(1), 6.
Impact factor: 6.525, SJR indicator: Q1 (Pharmaceutical Science)

VII. Martina Durcik, Ákos Nyerges, Žiga Skok, Darja Gramec Skledar, Jurij Trontelj, Nace Zidar, Janez Ilaš, Anamarija Zega, Cristina D Cruz, Päivi Tammela, Martin Welin, Yengo R Kimbung, Dorota Focht, Ondřej Benek, Tamás Révész, Gábor Draskovits, Petra Éva Szili, Lejla Daruka, Csaba Pál, Danijel Kikelj, Lucija Peterlin Mašič, Tihomir Tomašič (2021). New dual ATP-competitive inhibitors of bacterial DNA gyrase and Topoisomerase IV active against ESKAPE pathogens. European Journal of Medicinal Chemistry, 213, 113200.
Impact factor: 7.088, SJR indicator: Q1 (Drug Discovery)

VIII. Martina Durcik, Andrej Emanuel Cotman, Žan Toplak, Štefan Možina, Žiga Skok, Petra Eva Szili, Márton Czikkely, Elvin Maharramov, Thu Hien Vu, Maria Vittoria Piras, Nace Zidar, Janez Ilaš, Anamarija Zega, Jurij Trontelj, Luis A Pardo, Diarmaid Hughes, Douglas Huseby, Tália Berruga-Fernández, Sha Cao, Ivailo Simoff, Richard Svensson, Sergiy V Korol, Zhe Jin, Francisca Vicente, Maria C Ramos, Julia E A Mundy, Anthony Maxwell, Clare E M Stevenson, David M Lawson, Björn Glinghammar, Eva Sjöström, Martin Bohlin, Joanna Oreskär, Sofie Alvér, Guido V Janssen, Geert Jan Sterk, Danijel Kikelj, Csaba Pal, Tihomir Tomašič, Lucija Peterlin Mašič (2023). New Dual Inhibitors of Bacterial Topoisomerases with Broad-Spectrum Antibacterial Activity and In Vivo Efficacy against Vancomycin-Intermediate Staphylococcus aureus. Journal of Medicinal Chemistry. 66:6 pp. 3968-3994. , 27 p.
Impact factor: 8.039, SJR indicator: Q1 (Drug Discovery)

IX. Kaushik Nath Bhaumik, Anasztázia Hetényi, Gábor Olajos, Ana Martins, Réka Spohn, Lukács Németh, Balázs Jojart, Petra Szili, Anett Dunai, Pramod K Jangir, Lejla Daruka, Imre Földesi, Diána Kata, Csaba Pál, Tamás A Martinek (2022). Rationally designed foldameric adjuvants enhance antibiotic efficacy via promoting membrane hyperpolarization. Molecular Systems Design & Engineering 7:1 pp. 21-33. , 13 p.
Impact factor: 4.92, SJR indicator: Q1 (Biomedical Engineering)

X. Gábor Apjok, Mónika Számel, Chryso Christodoulou, Viktória Seregi, Bálint Márk Vásárhelyi, Tamás Stirling, Bálint Eszenyi, Tóbiás Sári, Fanni Vidovics, Erika Nagrand, Dorina Kovács, Petra Szili, Ildikó Ilona Lantos, Orsolya Méhi, Pramod K.

Jangir, Róbert Herczeg, Bence Gálik, Péter Urbán, Attila Gyenesei, Gábor Draskovits, Ákos Nyerges, Gergely Fekete, László Bodai, Nóra Zsindely, Béla Dénes, Ido Yosef, Udi Qimron, Balázs Papp, Csaba Pál & Bálint Kintses (2023). Characterization of antibiotic resistomes by reprogrammed bacteriophage-enabled functional metagenomics in clinical strains. Nature Microbiology 8:3 pp. 410-423. , 14 p.
Impact factor: 30.964, SJR indicator: D1 (Applied Microbiology and Biotechnology)

1. Introduction

1.1. The antibiotic resistance crisis

The discovery of antibiotics more than 90 years ago initiated a period of drug innovation and widespread implementation in healthcare and agriculture. They have provided an outstanding contribution to increase the life span by changing the outcome of several community-acquired and health care-associated bacterial infections, and they play a pivotal role in the success of some advanced medical practices (such as organ transplants and anti-cancer chemotherapy). Unfortunately, unlike most other drugs, antibiotics tend to lose their efficacy over time due to the emergence and dissemination of antibiotic resistance among bacterial pathogens.

The emergence of resistance traits to multiple classes of antibiotics, resulting in strains with multidrug-resistance (MDR) phenotypes, has progressively narrowed the available treatment options for many pathogens. In the case of some Gram-negative pathogens resistance developed for most or even all the available antimicrobial agents, resulting in extremely drug-resistant (XDR) or totally drug-resistant (TDR) phenotypes, which renders antibiotics unusable on certain infections, effectively recreating the challenges of the pre-antibiotic era. (Rossolini et al., 2014) Drug resistant bacterial infections are currently responsible for 700,000 worldwide deaths annually, and this number is predicted to rise up to 10 million by 2050, which would make antibiotic resistant infections the leading cause of death. (O'Neill, 2016)

Recent results show conclusively that antibiotic resistance is a natural phenomenon that predates the modern selective pressure of high-scale antibiotic usage. The emergence and dissemination of antibiotic resistance is driven by evolutionary processes that have provided the bacteria their outstanding ability to adapt to challenging environments for millennia. (Aminov, 2009; D'Costa et al., 2011) Resistance, in general, mainly can be mediated by two mechanisms: chromosomal resistance mutations or horizontal gene transfer via broad host-range plasmids. The relative importance of these mechanisms in resistance evolution is highly variable and depends on the antibiotic and the bacterial pathogens considered. (Hughes & Andersson, 2015) This dissertation is mainly concerned with inhibitors of the Topoisomerase IV - DNA gyrase complex

and against those antibiotics the relevance of plasmid-mediated resistance is much lower. Accordingly, the work focuses on chromosomal resistance mutations.

1.2. Challenges and perspectives in antibiotic development

The emergence of resistance puts antibiotic development efforts in a precarious position. Pharmaceutical research and development costs, which are estimated to be $400–$800 million per approved agent, combined with an estimated 95% failure rate, pose a considerable barrier to new drug development in general. (Payne et al., 2007; Spellberg et al., 2004) Additionally, due to the rise of drug-resistant bacteria, the commercial success of antibiotic development is unpredictable. The biggest challenge of antibiotic development is low profitability, which is often due to unsustainable low prices of the drug, short treatment courses and the need for conservation. As older antibiotics are still effective for treating most infections, the primary value of new antibiotics is to treat multidrug- resistant infections and provide a protective benefit against emerging pathogens. As the development of resistance is hastened by use, new antibiotics are stewarded as a last resort, which results in low sales. (Årdal et al., 2020) Paradoxically, as the need for new antibiotics is greater than ever, large pharmaceutical companies have mostly abandoned the market, accounting for only 4 of the 42 antibiotics currently under development. (Pew Charitable Trust, 2020; Jackson et al., 2018)

Consequently, the main driving force of current antibiotic development is the notion of finding ‘resistance-proof’ antibiotics. By principle, an antibiotic could be called such if resistance cannot evolve, because mutations that confer clinically significant resistance are exceedingly rare. (Bell & MacLean, 2018) Antibiotic combination therapy has long been suggested as a potential strategy to overcome rapid resistance evolution. The rationale for this theory is that multiple drugs with different modes of action generally require the simultaneous emergence of multiple different mutations at all target genes to achieve resistance. The simultaneous acquisition of multiple specific mutations is exceedingly rare. (Munck et al., 2014; Suzuki et al., 2015) Although successful in many cases, antimicrobial combination therapy suffers from several limitations, such as differences in the pharmacodynamics of the component antibiotics, elevated toxicity compared to monotherapy and potentially elevated risk for *Clostridium difficile* and fungal infections. (Tamma et al., 2012)

Antibiotics with multiple independent cellular targets is an emerging alternative. There are multiple mechanisms by which antimicrobial compounds may inhibit multiple bacterial targets. (Silver, 2007) In the case of hybrid drugs, two antibiotic pharmacophores with dissimilar targets are covalently linked to form one molecule. (Domalaon et al., 2018. Klahn & Brönstrup, 2017) Other antibiotics target two or more non-overlapping regions of a single bacterial protein and furthermore, equipotently inhibit two or more bacterial proteins. (Oldfield & Feng, 2014; Silver, 2007) Although it is a major focus of the pharmaceutical industry, designing multi-targeting antibiotics remains challenging. Until now, only a handful of antibiotic candidates displayed a balanced inhibition of multiple microbial targets. (Ince et al., 2002; Strahilevitz & Hooper, 2005; Tari et al., 2013) Additionally, due to the shortage of in-depth resistance studies, our knowledge on the tempo and mode of resistance development against multi-targeting antibiotics remains limited.

1.3. DIvERGE

To establish the resistance-proof nature of an antibiotic, it is essential to precisely estimate the rate of resistance evolution at the earliest stages of development. Unfortunately, standard microbial protocols are slow, have a low coverage, and may fail to predict the frequency and molecular mechanisms of antibiotic resistance by genomic mutations. The two most widespread methods, fluctuation tests and serial passage experiments, generally rely on spontaneous mutational processes and therefore can explore only a small fraction of the sequence space. (Bell & MacLean, 2018) This is especially problematic in examining potential resistance against multi-targeting antibiotics, where a high level of resistance demands the simultaneous acquisition of multiple, rare mutations, many of which seemingly provide little benefit individually.

Directed evolution with random genomic mutations (DIvERGE), a recently published genome engineering method from our laboratory, addresses the aforementioned shortcomings of current *in vivo* mutagenesis techniques. (Nyerges et al., 2018) DIvERGE enables mutagenesis of predefined long genomic regions with broad, controllable mutagenesis spectra for each nucleotide position. It also allows very high mutation rates of the target sequences, enables multiple rounds

of mutagenesis and selection, and is applicable to a range of host species without the need for prior genomic modification.

DIvERGE is based on a unique single-strand DNA oligonucleotide design strategy where long, continuous genomic segments are covered by the alignment of partially overlapping mutagenized DNA oligonucleotides. Tuning of the nucleotide composition in each synthetic oligonucleotide ensures that each possible mutation is represented in the synthesized pool. These oligonucleotide pools are synthesized using a soft-randomization protocol. (Hermes et al., 1989) In a nutshell, soft-randomization introduces a small amount of nucleotide mixture at specific variable positions of the wild type sequence. It thereby generates oligonucleotides with randomly positioned mutations. Moreover, soft-randomization enables the precise control of the rate and spectrum of mutations in the targeted segment.

The randomized oligonucleotides fully cover the locus of interest and induce mutagenesis at their target after incorporation. Prior works indicate that limiting the number of mismatches compared with the target sequence allows for an efficient genomic integration of oligonucleotides, while the overlapping design permits random and uniformly distributed mutagenesis along exceptionally long DNA segments. (Wang et al., 2011; Wang & Church, 2011)

Similarly to prior approaches, DIvERGE proceeds via cell growth, oligo delivery and incorporation and mutagenesis, leading to a highly elevated genetic diversity of the mutagenized population. The entirety of the process is illustrated by Figure 1.

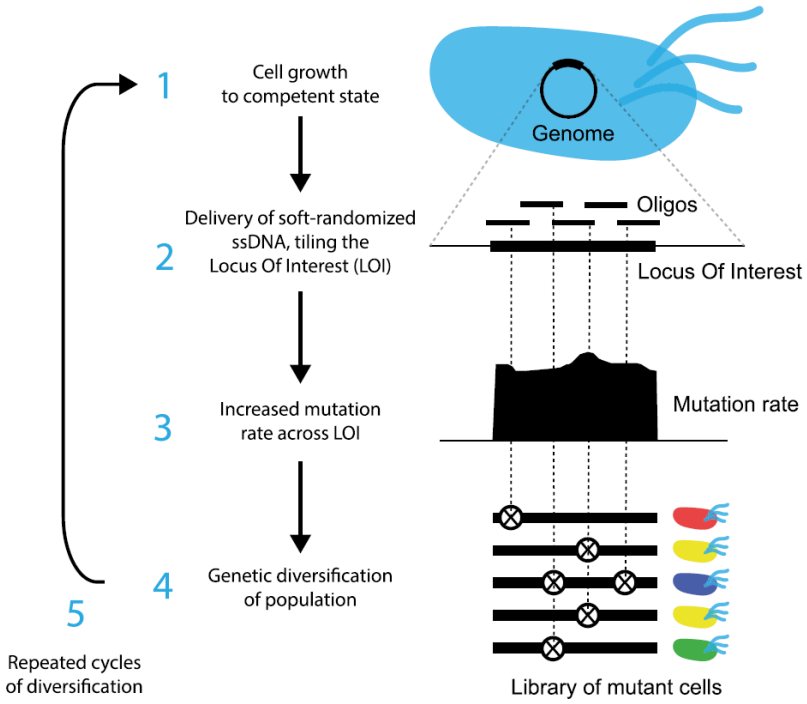

Figure 1. Overview of the DIvERGE method. Randomized DNA oligo synthesis precisely controls the rate of mutations via partially overlapping oligonucleotides. These oligonucleotides fully cover the locus of interest and induce mutagenesis at their target after incorporation. DIvERGE proceeds via cell growth (1), oligo delivery and incorporation (2), and mutagenesis (3), leading to a highly elevated genetic diversity of the mutagenized population (4).

1.4. The DNA gyrase and Topoisomerase IV complexes and their inhibitors

1.4.1. Structure and function

DNA gyrase and Topoisomerase IV protein complexes offer an exceptional target for developing multi-targeting antibiotics, because of the homology of their corresponding subunits and the substantial overlap in their three-dimensional protein structures. (Bisacchi & Manchester, 2015; Collin et al., 2011)

Both DNA gyrase and Topoisomerase IV are type II topoisomerases. In prokaryotes they form heterotetramers, with two subunits, GyrA-GyrB and ParC-ParE, respectively. Broadly speaking, the GyrA (ParC) subunit is involved with interactions with DNA, it contains the active-

site tyrosine responsible for DNA cleavage, and the B subunit contains the ATPase active site. (Champoux, 2001)

DNA gyrase and Topoisomerase IV are involved in breaking and rejoining double-stranded DNA, and thus, they determine changes in DNA topology during replication. The two complexes have complementary roles. All topoisomerases can relax supercoiled DNA, but only DNA gyrase can also introduce negative supercoils in a reaction that requires the hydrolysis of ATP, whereas Topoisomerase IV is mainly responsible for unlinking or decatenating DNA following DNA replication. (Champoux, 2001; Nöllmann et al., 2007)

Two main mechanisms are responsible for the antibacterial activity of drugs targeting DNA gyrase (or Topoisomerase IV). The first is the inhibition of the enzymatic activity, the second involves stabilization of the enzyme–DNA complex, or gyrase poisoning. It is gyrase poisoning that has been found to be the most effective mode of action of inhibitors of DNA gyrase and other topoisomerases. This is because relatively low occupancy of an inhibitor bound to its target can lead to sufficient protein-stabilized breaks in DNA to initiate a cascade of events that ultimately result in cell death. In bacteria, this is thought to involve chromosome fragmentation, the induction of the SOS response, and the production of reactive oxygen species. (Drlica et al., 2009)

1.4.2. Topoisomerase inhibitor antibiotics

Both DNA gyrase and Topoisomerase IV are clinically validated antibacterial targets and a substantial fraction of antibiotics currently used in clinical settings are inhibitors of them.

Quinolones and fluoroquinolones are by far the most successful antibacterials targeting DNA gyrase. The compounds originated from nalidixic acid, discovered by accident as a by-product during the synthesis of chloroquine. The first-generation quinolones, nalidixic acid and oxolinic acid have relatively weak antimicrobial activity, but the synthesis of the fluoroquinolones and their improvement over several generations, for example ciprofloxacin (second), levofloxacin (third) and moxifloxacin (fourth generation), has led to potent antibacterial compounds. (Emmerson & Jones, 2003) DNA gyrase is the primary target for quinolones in Gram-negative bacteria, but Topoisomerase IV is frequently the main target in Gram-positive organisms. (Hooper,

2003) The indicator of primary target is the site of point mutations that confer quinolone resistance. This tends to be largely restricted to discrete regions of gyrA and gyrB (or parC and parE, the equivalent topo IV genes) that are termed the quinolone-resistance-determining regions or QRDRs. (Yoshida et al., 1990, 1991) Unfortunately, clinically significant resistance against fluoroquinolones has already arisen in pathogenic bacteria. This is not unexpected, for two reasons. First, fluoroquinolones do not target the gyrase and topoisomerase complexes equipotently. (Hooper & Jacoby, 2015; Hooper & Jacoby, 2016) Second, low level of resistance against these antibiotics can readily emerge by mutations in efflux pumps and genes involved in transcription or translation. (Garoff et al., 2020)

Aminocoumarins, also referred to as coumarins, are compounds containing a 3-amino-4,7-dihydroxycoumarin ring. The aminocoumarins, novobiocin, clorobiocin and coumermycin A1, are natural products isolated from Streptomyces species; there are now also many derivatives made by genetic manipulation and by chemical synthesis.(Heide, 2009; Oblak & Solmajer, 2007) Known since the 1950's for their inhibitory properties on nucleic acid synthesis in bacteria, they inhibit gyrase-catalyzed supercoiling of DNA by competing with ATP for binding to GyrB. Because of the overlap between the ATP- and aminocoumarin-binding sites in GyrB, resistance to aminocoumarins that maps to gyrB is limited to amino acids that do not significantly affect the supercoiling activity of gyrase, as this enzyme is essential to survival. (Confreres & Maxwell, 1992; Sugino et al., 1978) Coumarins are potent inhibitors of DNA gyrase *in vitro*, but their poor activity against Gram-negative bacteria, mammalian cytotoxicity and poor solubility prevent them from being clinically successful drugs. The only moderately successful antibiotic from this group was novobiocin, but it was seldom used after the 1970s and was pulled from the market in 1999 due to treatment failure via spontaneous resistance development during therapy with novobiocin and severe toxic side effects. (Bisacchi & Manchester, 2015)

2. Goals

The body of this dissertation is based on two main scientific publications. In both, we focused on resistance against multi-targeting antibiotics, utilizing DIvERGE and traditional microbiological methods. In the first paper, we attempted to describe resistance against a novel topoisomerase inhibitor currently in clinical development, termed gepotidacin. (Szili et al., 2019) Based on the experiences gathered in this work, we later attempted to aid the early development of novel antibacterial compounds with potential multi-targeting activity. (Nyerges et al., 2020)

Gepotidacin (GSK2140944) is an exemplary candidate to study resistance evolution toward multi-targeting antibiotics. (Biedenbach et al., 2016; Flamm et al., 2017) It is a novel triazaacenaphthylene antibiotic candidate currently in phase 3 clinical trials and is expected to enter the clinical practice in the upcoming years. (Scangarella-Oman et al., 2020; Taylor, Morris, et al., 2018) The molecule inhibits bacterial DNA gyrase and Topoisomerase IV with a novel mode of action. Using a standard frequency of resistance test, early studies have failed to identify resistant clones of Neisseria gonorrhoeae and Escherichia coli against this new compound, suggesting that individual mutations cannot provide substantial resistance to gepotidacin. (Farrell et al., 2017; Nyerges et al., 2018) In our work, we demonstrated that contrary to expectations, reduced susceptibility to gepotidacin can evolve rapidly and previous works failed to identify resistance due to the limitations of the methods used.

In the second work, our collaborators have rationally designed a novel series of antibacterial compounds, endeavoring to achieve a balanced and simultaneous inhibitory effect on subunit B of DNA gyrase (GyrB) and subunit E of Topoisomerase IV (ParE). We characterized the biochemical and antibacterial properties, resistance development, as well as the *in vivo* efficacy of two representative compounds, termed ULD1 and ULD2.

3. Materials and Methods

3. 1. Media and antibiotics

For general growth of bacteria and electrocompetent cell preparation, lysogeny broth (LB) medium was used (10 g tryptone, 5 g yeast extract, 5 g sodium chloride per liter of water). For cell recovery after electroporation, we applied Terrific broth (TB; 24 g yeast extract, 12 g tryptone, 9.4 g K_2HPO_4, and 2 g KH_2PO_4 per liter of water). For antimicrobial susceptibility tests and selection of resistant variants, cation-adjusted Mueller-Hinton II broth (MHBII) was used. To prepare MHBII broth, 22 g of MHBII powder (Becton, Dickinson and Co.) was dissolved in 1 liter of water (3 g beef extract, 17.5 g acid hydrolysate of casein, and 1.5 g starch). MHBII agar was prepared by the addition of 14 g Bacto agar to 1 liter bacterial MHBII broth. Bacterial media were sterilized by autoclaving 15 min at 121°C. To distinguish lacZ knockout strains and wild type strains, sterile solutions of X-Gal (5-bromo-4-chloro-3-indolyl-β-D-galactopyranoside) and IPTG (isopropyl-β-D-1-thiogalactopyranoside) were added to the MHBII agar medium after autoclaving. The final X-Gal and IPTG concentrations in the medium were 40 mg/liter and 0.2 μM, respectively. Antibiotics and chemicals were ordered from Sigma-Aldrich (ampicillin, kanamycin, chloramphenicol, X-Gal, and IPTG), Fluka Analytical (ciprofloxacin), and MedChem-Express (gepotidacin).

3.2. Oligonucleotides

Oligonucleotides were synthesized at the Nucleic Acid Synthesis Laboratory of the Biological Research Centre of the Hungarian Academy of Sciences. Soft-randomized DIvERGE oligonucleotides were manufactured according to a previously described soft-randomization protocol (Nyerges et al., 2018). PCR primers were purified with standard desalting, while mutagenic oligonucleotides were purified with high-performance liquid chromatography (HPLC). Lyophilized oligonucleotides were dissolved in 1x Tris-EDTA (TE) buffer (pH 8) (Integrated DNA Technologies) at a final concentration of 100 μM. DIvERGE oligonucleotides were dissolved in 0.5x TE buffer at a final concentration of 500 μM. The dissolved oligonucleotides were stored at -

20°C. The sequence of all the oligonucleotides used are available in the File S1 of Szili et al, 2019. and file S1 Data of Nyerges et al., 2020.

3.3. Plasmid construction

To perform single-stranded DNA (ssDNA) recombineering and DIvERGE in *K. pneumoniae* ATCC 10031, we generated a novel version of pORTMAGE, termed pORTMAGE311B. This plasmid possesses a tightly regulated XylS-Pm regulator/promoter-based λ Beta and E. coli MutL E32K coexpression system. On pORTMAGE, the expression of MutL E32K of E. coli abolishes methyl-directed mismatch repair (MMR) during the time period of oligonucleotide incorporation into the bacterial genome (Nyerges et al., 2016). PORTMAGE311B ensured functionality at 37°C and the rapid inducibility of λ Beta and E. coli MutL E32K by the addition of 1 mM m-toluic acid as an inducer. The temporal coexpression of λ Beta and MutL E32K also limits off-target mutagenic effects on the course of genome editing. The construction of pORTMAGE311B was performed by introducing the coding sequence of the dominant E. coli mutL(E32K) allele to the pSEVA258beta plasmid (Ricaurte et al., 2018). To this aim, mutL(E32K) was PCR amplified from pORTMAGE2 (Nyerges et al., 2016) using the primers RBE32KF and XE32KR. The PCR product was then purified and digested with BamHI and XbaI. Next, the resulted fragment was cloned downstream of beta within pSEVA258beta. Finally, the successful assembly of the plasmid was verified by PCR and confirmed by capillary sequencing. pORTMAGE311B was also deposited to Addgene (no. 120418).

3.4. DIvERGE in *Klebsiella pneumoniae*

DIvERGE in *Klebsiella pneumoniae* ATCC 10031 was carried out according to a previously described DIvERGE workflow (Nyerges et al., 2018), with minor modifications. Briefly, *K. pneumoniae* cells carrying pORTMAGE311B plasmid were inoculated into 2 ml LB medium plus 50 μg/ml kanamycin and were grown at 37°C and 250 rpm overnight. From this starter culture, 500 μl stationary phase culture was inoculated into 50 ml LB medium plus 50 μg/ml

kanamycin and grown at 37°C under continuous shaking at 250 rpm. Induction was initiated at an optical density at 600 nm (OD_{600}) of 0.4 by adding 50 µl of 1M m-toluic acid (dissolved in 96% ethyl alcohol; Sigma-Aldrich). Induction was performed for 30 min at 37°C. After induction, cells were cooled on ice for 15 min. Next, cells were washed 3 times with 50 ml sterile ice-cold ultrapure distilled water. Finally, the cell pellet was resuspended in 800 µl sterile ultrapure distilled water and kept on ice until electroporation. To perform DIvERGE, and separately, the saturation mutagenesis of GyrA D82 and ParC D79, the corresponding gyrA- and parC-targeting oligonucleotides were equimolarly mixed at a final concentration of 500 µM, and 2 µl of this oligonucleotide mixture was added to 40 µl electrocompetent cells in 10 parallel samples. Following the electroporation of each sample, the 10 parallel samples were pooled, and immediately after electroporation, cells were suspended in 50 ml TB to allow for cell recovery. After a 1-hour recovery period at 37°C and 250 rpm, an additional 50 ml LB medium along with 50 µg/ml (final concentration) kanamycin was added. Next, cells were grown at 37°C and 250 rpm for 24 h. To select clones with reduced susceptibility to gepotidacin from this DIvERGE library, 500 µl cell library was spread to 6 µg/ml gepotidacin-containing MHBII agar plates, and the plates were incubated at 37°C for 48 h. Finally, 10 randomly selected colonies were analyzed by capillary sequencing (sequencing primers were oligonucleotides KPGA1F and KPGA1R, and KPPC1F and KPPC1R) from both antibiotic-selected cell libraries.

3. 5. Engineering isogenic *Klebsiella* strains carrying mutations associated with reduced susceptibility to gepotidacin and fluoroquinolones

To investigate mutational effects on antibiotic susceptibility and growth phenotypes, mutations and mutation combinations linked to reduced susceptibility to gepotidacin and ciprofloxacin were reconstructed in *K. pneumoniae* ATCC 10031. (Nyerges et al., 2016, 2018) Briefly, pORTMAGE recombineering was performed using pORTMAGE311B (Addgene no. 120418). One microliter of 100 µM the corresponding oligonucleotides or oligonucleotide mixtures was used for ssDNA recombineering in appropriate combinations to create mutations linked to reduced susceptibility to gepotidacin and ciprofloxacin. Following recombineering, cells were allowed to grow overnight in TB medium at 37 °C and 250 rpm. Next, variants carrying ciprofloxacin resistance-conferring mutations were selected on plates with LB plus 100 ng/ml

ciprofloxacin, while mutants carrying the GyrA D82N and ParC D79N mutation combination were selected on plates with MHBII plus 6 μg/ml gepotidacin agar. Cells carrying individual mutations associated with reduced susceptibility to gepotidacin were plated onto LB plus 50 μg/ml kanamycin agar. To obtain individual colonies, cultures from each recombineering population were diluted, and appropriate dilutions were spread to agar plates. Plates were incubated at 37°C, and individual colonies were genotyped by allele-specific PCR (using oligonucleotides KPA82ASF and KPA82ASR, and KPC79ASF and KPC79ASR). Finally, positive clones were confirmed by capillary sequencing of the oligonucleotide target region.

3.6. Antibiotic susceptibility testing

MICs were determined using a standard serial broth microdilution technique according to the CLSI guidelines (Wayne et al., 1993.). Briefly, bacterial strains were inoculated from frozen cultures onto MHBII agar plates and were grown overnight at 37°C. Next, independent colonies from each strain were inoculated into 1 ml of MHBII medium and were propagated at 37°C and 250 rpm overnight. In the cases of *Enterococcus* and *Streptococcus sp.*, cells were plated to BHI agar plates, and BHI broth was used to determine MICs. To perform MIC assays, 12-step serial dilutions using 2-fold dilution steps of the given antibiotic were generated in 96-well microtiter plates (Sarstedt 96-well microtest plate with lid, flat base). Antibiotics were diluted in 100 μl of MHBII medium. Following dilutions, each well was seeded with an inoculum of $5x10^4$ bacterial cells. Each measurement was performed in at least 3 parallel replicates. Also, to avoid possible edge effects at the edge of the microwell plate, side rows (A and H) contained only medium without bacterial cells. Following inoculations, the plates were covered with lids and wrapped in polyethylene plastic bags to minimize evaporation but allow for aerobic O_2 transfer. Plates were incubated at 37°C under continuous shaking at 150 rpm for 18 h in an Infors HT shaker. After incubation, the OD_{600} of each well on the microwell plate was measured using a Biotek Synergy 2 microplate reader. The MIC was defined as the antibiotic concentration which inhibited the growth of the bacterial culture, i.e., the drug concentration where the average OD_{600} increment of the three replicates was below 0.05. Expanded panel antibacterial spectrum of ULD1, -2, and comparator antibiotics were tested at IHMA Europe Sàrl (Switzerland) and at Eurofins Pharmacology

Discovery Services (Taiwan) in broth microdilution assays, according to the corresponding CLSI guidelines (Wayne et al., 1993.).

3.7. Frequency-of-resistance assay

To determine the spontaneous frequency-of-resistance, approximately 10^{10} cells from stationary-phase MHBII broth cultures of *S. aureus* ATCC 700699 and *S. aureus* ATCC 43300 were plated to antibiotic-containing plates according to a standard protocol to determine frequency-of-resistance (Bell & MacLean, 2018; Ling et al., 2015). Prior to plating, bacteria were grown overnight in MHBII medium at 37 °C, 250 rpm, collected by centrifugation, and washed once in equal volumes of MHBII broth. From this concentrated cell suspension (250 μL), approximately 10^{10} cells were then plated to each MHBII agarose plates. Using agarose instead of agar reduced drug-adsorption and improved the performance of the assay. Petri-dishes (145 mm) were filled with 40 mL MHBII agarose medium containing the selective drug at the desired concentration (i.e., 2×, 4×, 8×, 12×, and 16× MIC of each given antibiotic). All experiments were performed in at least 3 replicates. Plates were grown at 37 °C for 72 hours. Total CFUs were determined simultaneously in each experiment by plating appropriate dilutions to antibiotic-free MHBII agar plates. Finally, resistance frequencies for each strain were calculated by dividing the number of colonies formed after a 72-hour incubation at 37 °C by the initial viable cell count.

3. 8. Adaptive laboratory evolution

Adaptive laboratory evolution experiments followed an established protocol for automated laboratory evolution (Bódi et al., 2017; Lázár et al., 2018) and aimed to maximize the reached drug resistance during a fixed time period. At each transfer step, 10^7 bacterial cells were transferred to a new culture. Adaptation to ciprofloxacin was performed by passaging 6 independent populations of *Klebsiella pneumoniae* ATCC 10031 wild type, *Escherichia coli* K-12 MG1655 wild type, and *Escherichia coli* K-12 MG1655 ΔmutS strains in the presence of increasing antibiotic concentrations. Likewise, adaptation to ULD1, ULD2 and novobiocin was performed by passaging

10-10 independent lines of *Staphylococcus aureus* ATCC 43300 (MRSA) and *Staphylococcus aureus* ATCC 700699 (VISA) strains in the presence of increasing antibiotic concentrations. Experiments were conducted in 96-well plates in MHBII medium, utilizing a checkerboard layout to minimize and monitor cross-contamination. These 96-well deep-well plates (0.5 ml, polypropylene, V-bottom) were covered with sandwich covers (Enzyscreen BV) to ensure an optimal oxygen exchange rate and limit evaporation and were shaken at 150 rpm at 37°C. Twenty microliters of each evolving culture was transferred in parallel into four independent wells containing 350 µl fresh medium and increasing concentrations of gepotidacin and ciprofloxacin (i.e., 0.5x, 1x, 1.5x, and 2.5x the concentrations of the previous concentration step). Following cell transfer, each culture was allowed to grow for 48 h. At each transfer, cell growth was monitored by measuring the optical density at 600 nm (OD_{600}) (Biotek Synergy 2). Only populations with (i) vigorous growth (i.e., OD_{600} >0.25) and (ii) the highest drug concentration were selected for further evolution. Accordingly, only one of the four populations was retained for each independently evolving strain. This protocol was designed to avoid population extinction and to ensure that populations with the highest level of resistance were propagated further during evolution. Samples from each transfer were frozen in 15% dimethyl sulfoxide (DMSO) at -80°C for further analysis. Adaptation of an individual population was terminated when the antibiotic concentration in the given well would have exceeded 200 µg/ml after the transfer. Cells from these highly drug-resistant populations were frozen after the addition of 15% dimethyl sulfoxide (DMSO) and were kept at -80°C. Following adaptation, cells from each final population were spread onto MHBII agar plates, and individual colonies were isolated.

3.9. Capillary sequencing

Genotypes of the isolated clones from frequency-of-resistance assays, DIvERGE, as well as adaptive laboratory evolution experiments were checked by capillary sequencing. The drug-target regions of gyrA, gyrB, parC and parE genes were amplified by PCR using DreamTaq PCR 2X Master Mix (ThermoFisher Scientific): denaturation 95 °C, 3 minutes; 30 cycles: 95 °C, 30 seconds; 65 °C, 30 seconds; 72 °C, 1 minute; and final extension 72 °C, 3 minutes. The sequences of the corresponding PCR oligos are available in the supplementary files File S1 of Szili et al, 2019,

and file S1 Data of Nyerges et al., 2020. KPGA1F, KPGA1R were used to amplify gyrA from *K. pneumoniae* ATCC 10031 lines, KPPC1F, KPPC1R were used to amplify parE from *K. pneumoniae* ATCC 10031 lines, while 769B2F, SAGB1R were used to amplify gyrB from *Staphylococcus aureus* ATCC 700699 (VISA) lines and 769E2F, SAPE1R primers were used to amplify parE. PCR products were treated with ExoSAP-IT PCR Product Cleanup Reagent (ThermoFisher Scientific) for 15 seconds at 37 °C to hydrolyze excess primers and nucleotides. Samples were then subjected to capillary sequencing with the corresponding forward primer.

3.10. SMRT sequencing-based analysis of target-mediated resistance

Pooled *S. aureus* clones, isolated from first-step frequency-of-resistance assays, were subjected long-read amplicon sequencing. First, bacterial colonies were picked up from 2 independent FoR libraries. Clones were inoculated in 100 μL MHBII medium in 96-well microtiter plates and were grown overnight at 37 °C. Stationer-phase cultures were mixed equally, and genomic DNA was isolated using GeneElute Bacterial Genomic DNA Kit (Sigma-Aldrich). Drug-target regions with flanking DNA regions were amplified by PCR using Q5 High-Fidelity 2X Master Mix (New England BioLabs): denaturation 98 °C, 3 minutes; 20 cycles: 98 °C, 15 seconds; 62 °C, 25 seconds; 72 °C, 1 minute 20 seconds; final extension 72 °C, 3 minutes, by using barcoded amplification primers describen in file S1 Data of Nyerges et al., 2020. Following PCRs, amplicons were purified using DNA Clean & Concentrator Kit (Zymo Research), eluted in water, and their DNA concentration was checked by using a Qubit 4 fluorimeter. Finally, samples were subjected SMRT sequencing on a Pacific Biosciences Sequel instrument using Sequel Polymerase v3.0, SMRT cells v3, and Sequencing chemistry v3.0 (Norwegian Sequencing Centre, UiO, Oslo, Norway). After sequencing, raw circular-consensus SMRT sequencing reads were demultiplexed according to their corresponding barcodes by using Demultiplex Barcodes pipeline on SMRT Link v5.1.0.26412 (SMRT Tools 4 v5.1.0.26366). A minimum barcode score of 26 was used to identify high-quality barcodes. Following demultiplexing, sequencing reads were mapped to their corresponding reference sequences (i.e., gyrB and parE) by using bowtie2 2.3.4 37 (http://bowtie-bio.sourceforge.net/bowtie2) in “very-sensitive” mode, and the nucleotide composition was extracted for each nucleotide position within the target regions. Finally, genotype-frequencies at

each nucleotide position was quantified by measuring the distribution and ratio of nucleotide substitutions for each reference nucleotide position.

3.11. Whole genome sequencing of adapted lines

Following adaptive laboratory evolution of ciprofloxacin resistance in *K. pneumoniae* ATCC 10031 and *E. coli* K-12 MG1655, single colonies from three adapted lines were subjected to whole genome sequencing on an Illumina HiSeq 4000 platform. Samples were similarly prepared to *S. aureus* Mu50 ATCC 700699 under ULD2 stress, 6–6 random colonies (from spreading each 5 independently evolved lines on MHBII agar plates). Prior to sequencing, genomic DNA (gDNA) was isolated from each adapted line and the corresponding wild type strain by using the GenElute gDNA isolation kit (Sigma-Aldrich), according to the manufacturer's instructions. To perform DNA sequencing, sequencing libraries were constructed from the gDNAs by fragmenting samples to a mean fragment length of 300 bp. Next, sequencing libraries were prepared by using a TruSeq DNA PCR-free library prep kit (Illumina). Finally, sequencing libraries were sequenced on a single sequencing lane of an Illumina HiSeq 4000 system using a HiSeq 3000/4000 SBS kit (300 cycles, FC-410-1003; Illumina) to generate 2x150-bp paired-end reads. Following sequencing, in order to determine the variants and to annotate the mutations, we mapped sequencing reads to their corresponding reference genomes with the mem subcommand of bwa 0.7.12-r1039 (Burrows-Wheeler Aligner (Li & Durbin, 2009)). The single-nucleotide polymorphisms (SNPs) and indels were called with VarScan v2.3.9 (Koboldt et al., 2012) with the following parameters: min-reads2=4, min-coverage=30, min-var-freq=0.1, min-freq-forhom=0.6, min-avg-qual=20, strand-filter=0. Only variants with prevalence higher than 60% were voted as mutations. Following variant calling, mutations were also manually inspected within the aligned reads, and adapted lines that become hypermutators (i.e., that are accumulated more than 55 mutations in a single lineage) were excluded from further analysis. Finally, the annotation of each mutation with genomic features was performed with the intersect subcommand of bedtools v2.25.0 (Quinlan & Hall, 2010).

3.12. Fitness measurements

We observed the growth phenotype of bacterial variants by assessing their growth at 37 °C in antibiotic-free BHI medium following established protocols (Warringer & Blomberg, 2003). To measure growth, we inoculated 5×10^4 cells from early stationary-phase cultures (prepared in MHBII medium) into 100 μL of BHI medium in a 96-well microtiter plate and monitored growth for approximately 48 hours. Bacterial growth was measured as the OD_{600} of cultures at any given time point. OD_{600} measurements were carried out every 5 minutes using BioTek Synergy 2 microplate reader while bacterial cultures were grown at 37 °C under continuous shaking. Each bacterial variant and their corresponding wild types were measured in 6 replicates. Finally, growth rates were calculated from the obtained growth curves according to a previously described procedure. Fitness was approximated by calculating the area under curve (AUC) (Hasenbrink et al., 2005). AUC has been previously used as a proxy for fitness because it has the advantage to integrate multiple fitness parameters, such as the slope of exponential phase (i.e., growth rate) and the final biomass.

3. 13. Competition-based fitness measurements.

Competition assay-based fitness measurements were carried out by competing mutant strains against their corresponding wild type strain carrying a lacZ knockout mutation. The lacZ knockout strain was constructed by integrating a premature stop codon in place the 23rd amino acid of LacZ with a previously reported pORTMAGE protocol (Nyerges et al., 2016). Briefly, heat-induced pORTMAGE3 (Addgene no. 72678) containing *Klebsiella pneumoniae* ATCC 10031 cells were electroporated with KpLacZW23* oligonucleotide (2.5μM final concentration). Following oligonucleotide integration into the bacterial chromosome, lacZ-deficient variants were identified by plating cells out to X-Gal plus IPTG-containing MHBII agar plates at appropriate dilution to form single colonies, where knockout mutants formed white colonies and could be easily distinguished from the dark-blue colonies of the wild type containing a functional β-galactosidase gene. Each competition experiment started by inoculating early stationary-phase cultures in a 99:1 mutant-to-wild-type ratio into 10 ml MHBII medium at a 1:1,000 dilution and incubating each

culture at 37°C for 24 h under a constant agitation of 250 rpm. These cultures were then serially transferred into 10 ml fresh MHBII medium in a 1:1,000 dilution every 24 h for 3 subsequent transfers. To analyze the composition of each population, cultures were plated onto MHBII agar plates supplemented with X-Gal and IPTG (in 145 by 20-mm petri dishes; Greiner Bio-One Ltd.) at appropriate dilutions to obtain approximately 1,000 colonies per each plate. The plates were then incubated at 37°C overnight. The ratio of the mutant (lacZ proficient, blue colonies) and the wild type (lacZ deficient, white colonies) at each given time point was determined from the number of blue and white colonies on X-Gal plus IPTG agar plates. Importantly, prior experiments showed that lacZ-deficient *K. pneumoniae* cells suffer no competitive disadvantage compared to their corresponding wild type strain. Competition experiments were performed in five replicates. Finally, selection coefficients were estimated as the slope of the change in ratio, as defined in the following equation:

$$\ln[x_1(t)/x_2(t)] = \ln[x_1(0)/x_2(0)] + st$$

where s is the selection coefficient, t is time or number of generations, and x_1 and x_2 are the ratios of the two strains at a given time point (Dykhuizen, 1990; Karcagi et al., 2016).

3.14. Prevalence of mutations associated with reduced susceptibility to gepotidacin in sequence databases

In order to investigate if genotypes GyrA D82N and ParC D79N exist in bacteria, we downloaded all DNA sequences from the NCBI nucleotide database by using the following query: ftp://ftp.ncbi.nlm.nih.gov/blast/db/nt.??.tar.gz in wget 1.17.1 on 9 October 2018. We performed the BLAST search with tBLASTn 2.231 (Altschul et al., 1990) (build 7 January 2016) on the downloaded full-nucleotide database as the subject and GyrA and ParC as the query. The protein sequences of GyrA (GenPept accession no. P0AES4) and ParC (GenPept accession no. P0AFI2) were downloaded from UniProt. To perform BLAST, the database was fragmented, and the BLAST search was carried out on these smaller data sets (with argument max_target_seqs = 20,000). Separately obtained results were merged. Finally, for each sequence, the taxonomy of the source bacteria was assigned with blastdbcmd (version 2.2.31).

3.15. *S. aureus* dermal infection model

The testing strains, *S. aureus* USA300 (MRSA) BAA1556, *S. aureus* ECL2963646 (VRSA), and *S. aureus* Mu50 (VISA) ATCC 700699 were obtained from frozen stocks and thawed at room temperature. Next, an aliquot of 0.2 mL from each stock was transferred to 20 mL BHI broth and incubated at 37 °C with shaking (120 rpm) for 8 hours. Cells in 20 mL culture were pelleted by centrifugation, 3,500 g for 15 minutes, and then resuspended in 10 mL cold PBS, then cells were diluted in PBS to obtain the inoculum sizes of 1×10^5 or 1×10^6 CFU/mL, based on the testing strain's virulence. In all cases, the actual colony counts were determined by plating dilutions in at least 3 replicates onto MHBII agar plates followed by 24 hours' incubation and colony counting.

For dermal infections, groups of 5 female ICR mice weighing 24 ± 4 g, provided by BioLasco Taiwan (under a Charles River Laboratories Technology Licensee), were used. Animals were acclimated for 3 days prior to use and were confirmed to be in good health. Prior to infection, animals were anesthetized with etomidate-lipuro emulsion (20 mg /10 mL) at 20 mg/kg by IV injection, and then the fur on the back was removed by an electric shaver, and the epidermal layer was disrupted with an abrasive paper according to the protocol developed by Kugelberg and colleagues (Kugelberg et al., 2005). Mice were inoculated topically on the wound area with testing strain suspension, 5 μL/mouse. The target inoculation densities were 1×10^5 or 1×10^6 CFU/mL, based on the corresponding strain's virulence. Following infection, animals were housed separately. Prior to treatment, ULD1 and −2 were dissolved in 100% DMSO and then further diluted in either corn oil (90% corn oil + 10% DMSO in the final ointment) or 0.5% water-based carboxymethyl cellulose (CMC) solution. Test articles were administered topically (20 μL/mouse) twice daily. One no-treatment group was euthanized at 1 hour after infection for initial bacterial counts, and the other treatment groups were dosed twice daily with the test compounds and sacrificed either at 25 hours or at 73 hours postinfection. Animals were euthanized with CO_2 asphyxiation and the infected skin, a 2 cm^2 area, was excised. The skin samples of the wound infection (around 2 cm^2 areas) were then homogenized in 1 mL PBS (pH 7.4) with a polytron homogenizer. A 0.1 mL aliquot of each homogenate was used for serial 10-fold dilutions and plated onto MHBII agar plates for bacterial enumeration. Statistical significance ($P < 0.05$) was assessed with 1-way ANOVA followed by Dunnett's method. A significant ($P < 0.05$) decrease in the

bacterial counts of the treated animals compared with the vehicle control group was considered significant antimicrobial activity.

3.16. Mouse thigh infection models

Murine thigh infections for *Klebsiella pneumoniae* ATCC 10031 and *Staphylococcus aureus* Mu50 ATCC700699 were performed according to a previously established protocol (DeRyke et al., 2007; Tan et al., 2012). Experiments were performed on female CD-1 mice (Charles River Laboratories, USA). Bacterial cultures were prepared by inoculating single bacterial colonies into 5 ml of MHBII broth and were incubated at 37°C for 16 h under constant agitation (250 rpm). Next, 1⁄2 volume of a 50% (vol/vol) glycerol-water mixture was added to each culture, and 550 µl of these cell suspensions was frozen at -80°C. Before inoculation, cell suspensions were allowed to thaw at room temperature for 15 min. As test animals, groups of 5 female specific-pathogen-free ICR (CD-1) mice weighing 22±2 g were used. Animals were immunosuppressed by two intraperitoneal injections of cyclophosphamide, the first at 150 mg/kg of body weight 4 days before infection (day -4) and the second at 100 mg/kg 1 day before infection (day -1). On day 0, animals were inoculated intramuscularly into the right thigh with 10^6 CFU/mouse of *Klebsiella pneumoniae* ATCC 10031 or $6.0x10^5$ of *Staphylococcus aureus* Mu50 ATCC 700699 (0.1 ml culture/thigh). Prior to infection, ULD1 was formulated by dissolving the compound in 5% DMSO, 5% cremophor EL, and 50 mM potassium phosphate. Test agent was then dosed via IV administration at 2, 8, 14, and 20 hours post infection. Beginning at 2 hours post infection mice were dosed with either test article or positive control antibiotic. Mice receiving test agents were dosed intravenously at 10 mL/kg. Linezolid was delivered as a subcutaneous dose. Four animals were dosed per group. One group of 4 mice were euthanized at initiation of therapy (T = 2 hours) and CFUs determined. All remaining mice were euthanized at 26 hours 26 h after inoculation, animals were humanely euthanized with CO_2 asphyxiation, and then the muscle of the right thigh was harvested from each test animal. The removed muscle was homogenized in 3 ml of phosphate-buffered saline (pH 7.4) with a polytron homogenizer. Finally, 0.1 ml of these homogenates was used for serial 10-fold dilutions and plated onto LB agar for colony count (CFU per Gram) determination.

3.17. Ethics statement

All aspects of this work, including housing, experimentation, and animal disposal, were performed in general accordance with the Guide for the care and use of laboratory animals (Guide for the care and use of laboratory animals, 2011). All experiments were performed under animal biosafety level 2 (ABSL2) conditions with the oversight of veterinarians to ensure compliance with IACUC regulations and the humane treatment of laboratory animals. Animal experiments for this study were performed by Eurofins Panlabs Taiwan Ltd. The Institutional Animal Care and Use Committee (IACUC) reviewed the planned experiments submitted under Protocol Number IM003-01132016 and provided official approval. The company also obtained an Animal Welfare Assurance (identification number A5890-01) from the Department of Health & Human Services.

4. Results

4.1. Directed evolution accurately predicts the positions and impact of resistance mutations with strong synergism

Prior studies have demonstrated that gepotidacin selectively inhibits both bacterial DNA gyrase and Topoisomerase IV by a unique mechanism. Therefore, we subjected the four potential target genes to a single round of directed evolution with random genomic mutation (DIvERGE) mutagenesis in clinically relevant pathogen *Klebsiella pneumoniae*. We focused our efforts on *Klebsiella pneumoniae*. According to the WHO, infections caused by multidrug-resistant *Klebsiella* strains are emerging as a top-ranked challenge in the healthcare sector. (Tillotson, 2018) After mutagenesis with DIvERGE, we subjected the mutant library to gepotidacin stress, followed by sequencing of the isolates with resistance. As gepotidacin has not yet entered clinical use and, thus, its clinical breakpoint is not established, we defined resistance to gepotidacin as the MIC value that is equal or higher than the peak plasma concentration of the drug (9 μg/ml). (Taylor, Morris, et al., 2018) Amino acids D82 within the GyrA subunit and D79 of the ParC subunit are found to be mutated in all the clones isolated, and no further mutations have been found. Subsequent saturation mutagenesis of the two mutational hot spots has proven that the combination of two specific mutations (GyrA D82N and ParC D79N) is responsible for a high-level reduction of susceptibility to gepotidacin.

Next, we have studied the individual and combined effects of these mutations on susceptibility. For this purpose, the mutations were inserted individually into the genome of *K. pneumoniae* ATCC 10031. The double mutants were found to display as high as 2,080-fold reductions in gepotidacin susceptibility levels compared to the corresponding wild type strain of *K. pneumoniae*. (Table 1A) In contrast, the single mutants were found to show no considerable changes in gepotidacin susceptibility. These findings are consistent with prior single-step resistance selection studies that failed to recover mutants with significant resistance. (Farrell et al., 2017; Nyerges et al., 2018)

A.) Mutations associated with gepotidacin resistance		
Strain	**MIC (µg/ml)**	
	Gepotidacin	**Ciprofloxacin**
Wild type	0.063	0.004
GyrA D82N mutant	0.5	0.063
ParC D79N mutant	0.125	0.008
GyrA D82N; ParC D79N mutant	256	0.063
B.) Mutations associated with ciprofloxacin resistance		
Strain	**MIC (µg/ml)**	
	Gepotidacin	**Ciprofloxacin**
Wild type	0.063	0.004
GyrA S83F mutant	0.5	0.08
GyrA S83F, D87G mutant	0.25	0.125
GyrA S83F, D87G; ParC S80I mutant	0.063	2
GyrA S83F, D87G; ParC S80I, E84G mutant	0.31	4

Table 1. Gepotidacin and ciprofloxacin MICs of single-step mutations and their combination in *Klebsiella pneumoniae* ATCC 10031

4.2. No substantial fitness cost of gepotidacin resistance

Antibiotic resistance typically induces a fitness cost in the form of reduced bacterial growth rates, and such costs shape the long-term stability of antibiotic-resistant populations. (Hughes & Andersson, 2015; Sommer et al., 2017) Therefore, we have investigated the fitness effects of target-mediated resistance to gepotidacin in *K. pneumoniae*. To this aim, we have studied the wild type and mutant *K. pneumoniae* strains carrying mutations associated with resistance to gepotidacin or fluoroquinolones. The mutations causing fluoroquinolone resistance are widespread in clinical isolates and affect the same genes (namely, gyrA and parC); therefore, they provide a benchmark to estimate the fitness costs compared to the wild type strain. (Chen et al., 2003; Krapp et al., 2018)

Relative fitness was estimated by pairwise competition experiments between the wild type strain and a specific mutant strain in nutrient-rich antibiotic-free bacterial medium (Mueller-Hinton II broth [MHBII]) at 37°C. We have found that the mutation combination of GyrA D82N and ParC D79N, which confers resistance to gepotidacin, significantly decreases fitness in *K. pneumoniae*. However, the fitness cost of gepotidacin resistance-causing mutations is comparable to the fitness cost of mutations associated with clinically relevant fluoroquinolone resistance. Importantly, the ParC D79N mutation is found to confer no measurable fitness cost individually (Figure 2A). Our findings remained the same when active human blood serum was added to the medium (data not shown).

We next investigated whether mutants with resistance to gepotidacin display reduced virulence *in vivo*. As drug resistant *K. pneumoniae* is frequently responsible for wound and systemic infections, we have studied a murine thigh wound infection model. (Tan et al., 2012; Velkov et al., 2013) Specifically, we have examined the wound colonization capacity of the wild type strain, as well as that of representative *K. pneumoniae* mutants with gepotidacin or ciprofloxacin resistance. For this purpose, the wild type strain and each isogenic mutant strain were inoculated into the thigh tissue of female ICR mice (each treatment group contained 5 animals). After 26 h, bacterial colonization was determined by plating thigh tissue homogenates to MHBII agar plates. No significant decrease in *in vivo* virulence was observed for any of the mutants compared to the wild type strain (Figure 2B).

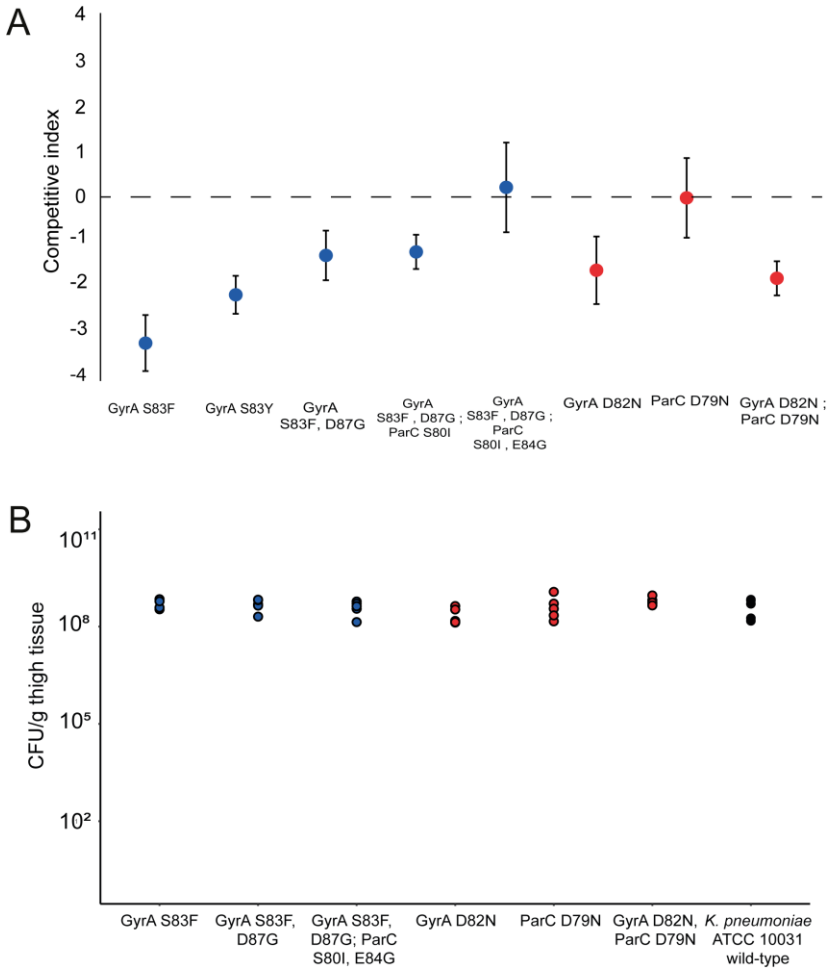

Figure 2. Fitness cost and virulence of bacteria with resistance to gepotidacin. (A) *In vitro* competition between mutant and wild type *Klebsiella pneumoniae*. Isogenic mutants of *Klebsiella pneumoniae ATCC 10031* carrying either a mutation or mutation combination conferring resistance to gepotidacin (red), or clinically occurring fluoroquinolone resistance-associated mutations (blue) competed against the wild type strain. In competition assays, a competitive index of <0 indicates that the wild type population outcompetes the mutant population, and conversely, a competition index of >0 indicates that the mutant population outcompetes the wild type population. Error bars indicate the standard deviation (SD) based on five biological replicates. (B) Virulence of *Klebsiella pneumoniae* mutants and the wild-type strain in a murine thigh infection model. Shown are the bacterial burdens in infected thigh tissues after 26 h of infection caused by wild type *Klebsiella pneumoniae* ATCC 10031 (black) or isogenic mutants carrying either mutation or mutation combination conferring resistance to gepotidacin (red), or clinically occurring mutations associated with fluoroquinolone resistance (blue). The bacterial burden was assayed in CFU per Gram of

tissue (n=5 animals per data point, see Materials and Methods for details). No mutants were found to display a significant difference in virulence compared to the wild type strain (t test, $P < 0.05$ for all pairwise comparisons).

4.3. Cross-resistance between ciprofloxacin and gepotidacin may drive the spread of gepotidacin resistance

Several prior works demonstrate that certain resistance mutations may be present in bacterial populations long before being exposed to a given antibiotic. Based on this knowledge, we hypothesized that prolonged use of other antibiotics might select for mutations that serve as stepping stones toward resistance to gepotidacin. The most likely antibiotic family for this purpose would be fluoroquinolones, as they are widely employed in clinical practice, and share a target with gepotidacin in the DNA gyrase – TTopoisomerase IV complex. The putative binding sites of gepotidacin and fluoroquinolones on the GyrA protein are adjacent to each other, separated by only a single amino acid. (Collin et al., 2011; Hooper & Jacoby, 2016; Wohlkonig et al., 2010) Despite the functional similarities between these drug classes, a prior paper reported that fluoroquinolone-resistant clinical isolates displayed no cross-resistance to gepotidacin. (Flamm et al., 2017)

To reinvestigate this issue, we have focused on ciprofloxacin, a widely employed and well-characterized fluoroquinolone drug. Several ciprofloxacin resistance-conferring mutations and mutation combinations in clinical isolates provide no relevant cross-resistance against gepotidacin (Table 1B). On the contrary, we have found that the GyrA D82N single-mutant strain displays an over 16-fold increase in ciprofloxacin resistance level compared to that of the wild-type *K. pneumoniae* ATCC 10031 strain. Remarkably, the same mutation confers only a 2-fold increase in gepotidacin MIC level. As might be expected, the GyrA D82N and ParC D79N double mutants also display significant resistance to ciprofloxacin (Table 1A). This finding raise the possibility that the D82N mutation of GyrA might be present in fluoroquinolone-resistant clinical isolates, increasing the likelihood of the subsequent emergence of double mutants with resistance to gepotidacin. To prove this theory, we did a systematic sequence search on the prevalence of the GyrA D82N and ParC D79N mutations in currently available sequence databases (as of 9 October 2018). It has revealed that both mutations occur in a wide range of Gram-negative and Gram-

positive bacteria, including fluoroquinolone resistant clinical isolates of *E. coli* (Correia et al., 2017) and other species belonging to the *Salmonella, Mycoplasma, Clostridium, Citrobacter, Streptococcus*, and *Neisseria* genera. *Neisseria* and *Streptococcus* are especially clinically relevant in this context, as infections caused by these bacteria are reported to be the targets of gepotidacin in recent clinical trials. (O'Riordan et al., 2017; Scangarella-Oman et al., 2020; Taylor, Morris, et al., 2018) These results indicate that several clinically occurring human pathogens require only a single extra mutation to evolve highly reduced susceptibility to gepotidacin.

To establish further that ciprofloxacin promotes reduced susceptibility to gepotidacin, we have performed adaptive laboratory evolution under ciprofloxacin stress with wild type *K. pneumoniae* ATCC 10031, as well as the wild type and *ΔmutS* hypermutator strains of *E. coli* K-12 MG1655. According to established protocols in literature and our laboratory (Bell & MacLean, 2018; Lázár et al., 2018; Martínez et al., 2007), six parallel evolving populations of each strain were exposed to gradually increasing concentrations of ciprofloxacin. The experimental setup aimed to maximize the level of drug resistance evolving in the populations during a fixed time period, approximately 116 generations in our case. In line with previous clinical and laboratory studies, ciprofloxacin resistance was seen to emerge quickly in our experiments (Baym et al., 2016; Hooper & Jacoby, 2016) (Fig. 3A), especially in *ΔmutS* hypermutator lineages. Despite the short time frame, all *E. coli* and *K. pneumoniae* populations reached ciprofloxacin resistance levels equal to or above the EUCAST clinical breakpoint (Breakpoint tables for interpretation of MICs and zone diameters, 2019.) (Fig. 3A and B). Three randomly selected ciprofloxacin-resistant lineages per strain were selected for gepotidacin MIC measurements. Strikingly, all have been found to display a >64- to 1,058-fold increase in gepotidacin resistance compared to the corresponding control strains (Fig. 3B). We also carried out whole genome sequencing of 2 and 3 evolved lineages derived from *E. coli* K-12 MG1655 and *K. pneumoniae* ATCC 10031, respectively. Although these lineages display markedly reduced gepotidacin susceptibilities (Fig. 3B), they do not carry mutations at GyrA D82 or ParC D79, suggesting that multiple other mutations may also select for reduced susceptibility to gepotidacin. Indeed, whole-genome sequencing has revealed that these ciprofloxacin-resistant lineages carry putative resistance mutations in genes involved in membrane efflux (acrR, soxR, and marR) and the general stress response (cusS and rpoB). Overall, these results strongly suggest that long-term exposure to ciprofloxacin stress promotes reduced susceptibility to gepotidacin.

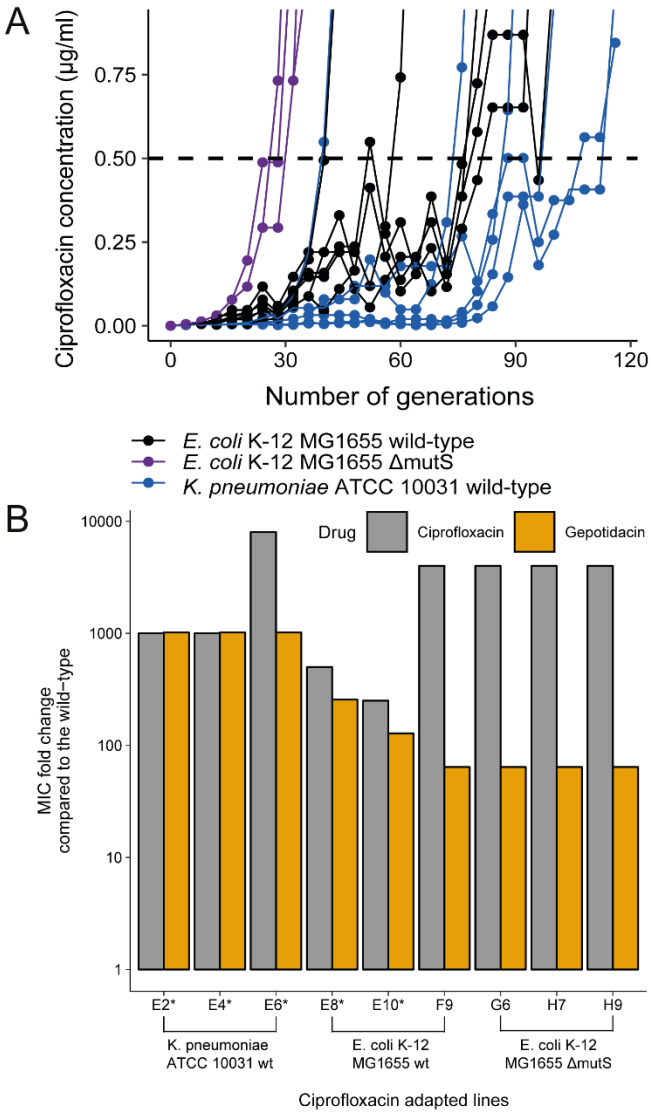

Figure 3. Adaptive laboratory evolution of *Klebsiella pneumoniae* and *Escherichia coli* under ciprofloxacin stress. (A) Antibiotic concentrations at which *K. pneumoniae* ATCC 10031 as well as *E. coli* K-12 MG1655 wild-type and *ΔmutS* hypermutator strains were able to grow under increasing ciprofloxacin stress as a function of time (number of cell generations). Dashed line represents the clinical breakpoint of ciprofloxacin resistance according to EUCAST. (B) Relative resistance level of the evolved lines against ciprofloxacin (gray bars) and gepotidacin (yellow bars) compared to the wild type at the end of the adaptive laboratory evolution. Asterisk (*) indicates that the evolved line was subjected to whole genome sequencing to uncover mutational processes behind the reduced susceptibility.

4.4. Novel dual-targeting DNA gyrase- Topoisomerase IV inhibitors ULD1 and ULD2 show improved bioactivity against clinically relevant pathogens

Our collaborators (Peterlin lab, University of Ljubljana) have recently discovered a novel class of DNA gyrase inhibitors with a pyrrolamidobenzothiazole scaffold, inspired by the marine natural product oroidin. (Gross et al., 2003; Tomašič et al., 2015) Most compounds from the published series primarily act on the bacterial DNA gyrase complex only and possess weak antibacterial activity. To transform these molecules into broadly effective antibiotics, they have executed modifications at several sites on the pyrrolamidobenzothiazole-6-carboxylic acid scaffold based on the co-crystal structure with subunit B of DNA gyrase and molecular dynamics (MD) simulations. The molecular modifications were aimed at designing novel inhibitors that display equipotent dual-targeting activity towards subunit B of DNA gyrase (GyrB) and subunit E of Topoisomerase IV (ParE), by a simultaneous establishment of strong interactions with multiple, functionally essential amino acids of both target proteins. The chemical modifications have yielded 2 antibiotic leads, ULD1 and ULD2.

When characterizing the bioactivity of these two molecules, first we have determined the minimum inhibitory concentrations (MICs) of ULD1 and ULD2 against a panel of Gram-negative and Gram-positive clinical pathogens (Table 2). ULD1 and ULD2 were found to display potent antibacterial activity against ESKAPE pathogens (*S. aureus, Enterococcus sp., Pseudomonas aeruginosa, Klebsiella pneumoniae, Acinetobacter baumannii), Streptococcus sp., and Clostridium difficile.* The MIC values against all studied multidrug-resistant *Staphylococcus*, *Enterococcus*, and *Streptococcus* isolates were below 2 μg/mL. Notably, ULD1 and ULD2 exerted activity against all MRSA, VRSA (MRSA/VRSA: methicillin-resistant/vancomycin-resistant *S. aureus),* and vancomycin-resistant *Enterococcus* (VRE) isolates, which frequently cause difficult-to-treat skin and soft-tissue infections (SSTIs). (Ramakrishnan et al., 2015) We hypothesize that further chemical modifications of ULD1/ULD2 could increase the potency of this compound class to inhibit Gram-negative pathogens as well.

Species and strain	Acquired resistance	ULD1	ULD2
		MIC (μg/mL)	
Staphylococcus aureus ATCC 700699 (Mu50, NRS1)	MRSA (SCC*mec* type II), VISA, Clindamycin-R, Daptomycin-NS, Erythromycin-R, Gentamycin-R, Imipenem-R, Levofloxacin-R, Oxacillin-R	0.0625	≤0.03125
Staphylococcus aureus ECL 2963646	MRSA, VRSA, Clindamycin-R, Erythromycin-R, Gentamycin-R, Levofloxacin-R	0.125	≤0.03125
Staphylococcus epidermidis ATCC 51625	MRSE, Oxacillin-R	0.0625	≤0.03125
Enterococcus faecalis ATCC 51575	VRE (VanB+), Clindamycin-R, Erythromycin-R, Gentamycin-R, Linezolid-IR, Mupirocin-R, Streptomycin-R	0.0625	≤0.03125
Enterococcus faecium BAA-2320	VRE (VanA+), Ampicillin-R, Ciprofloxacin-R, Clindamycin-R, Erythromycin-R, Levofloxacin-R, Imipenem-R, Teicoplanin-R	0.25	≤0.03125
Neisseria gonorrhoeae CCUG 57598	Cefoxitin-R, Ciprofloxacin-R, Linezolid-R, Tetracycline-R, Penicillin-R	≤0.03125	≤0.03125
Haemophilus influenzae ATCC 49247	Ampicillin-R, Vancomycin-R, Tetracycline-R	≤0.03125	0.125
Clostridium difficile BAA-1875	toxigenic, ribotype 078, Ertapenem-IR, Imipenem-R	≤0.03125	≤0.03125
Listeria monocytogenes ATCC 19111		0.125	0.125
Acinetobacter baumannii ATCC 19606		2	0.5
Klebsiella pneumoniae ATCC 10031		1	4
Pseudomonas aeruginosa ATCC 27853		8	2

Table 2. Antimicrobial activities of ULD1 and ULD2 against selected pathogenic bacteria. MIC measurements were performed in three replicates according to CLSI guidelines. Table legend: -R represents resistant, -NS represents non-sensitive, MRSA/VRSA: methicillin-resistant/vancomycin-resistant *S. aureus*, VISA: vancomycin-intermediate *S. aureus*, MRSE: methicillin-resistant *S. epidermidis*, VRE: vancomycin-resistant *Enterococcus*.

Encouraged by the excellent bioactivity of the molecules in MRSA and VRSA strains, we have focused on determining the antibacterial activity of ULD1 and ULD2 against a geographically and genetically diverse set of *S. aureus* clinical isolates, including 56 MRSA and 28 vancomycin-

intermediate and vancomycin-resistant strains, inclusive of recent clinical isolates. A large fraction of these isolates were simultaneously resistant to multiple other available antibiotics too. In sharp contrast to other approved antibiotics against staphylococcal infections, both ULD1 and ULD2 were found to exert a potent activity against all tested isolates (MIC ≤ 1 μg/mL, Fig 4).

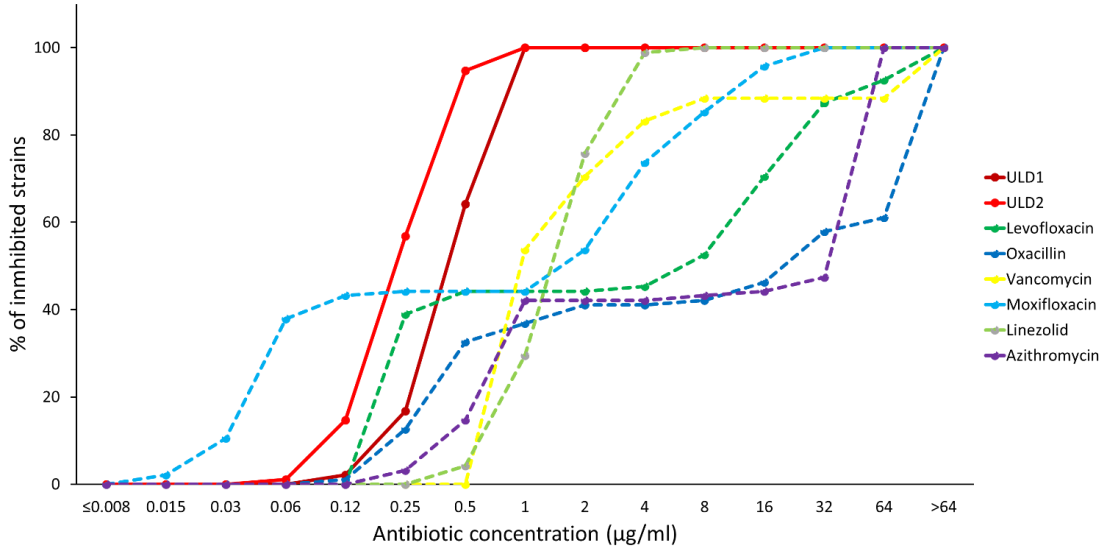

Figure 4. Antibacterial activities of ULD1 and ULD2. Antibacterial activities of ULD1 and ULD2 against a panel of 95 *S. aureus* clinical isolates. Strains included 55 MRSA and 28 vancomycin-intermediate or -resistant isolates with diverse geographic origins. All strains (100%) were inhibited at 1 μg/mL concentration of ULD1 and ULD2. MICs were determined via broth microdilution according to CLSI guidelines.

4.5. Resistance against ULD1 and ULD2 is limited and requires mutations at both targets

Antibiotics with a single molecular target are usually prone to resistance development induced by spontaneous mutations, while theoretically multi-targeting antibiotics are less vulnerable to resistance, as the simultaneous acquisition of multiple, specific mutations is exceedingly rare. (Bell & MacLean, 2018; Oldfield & Feng, 2014; Silver, 2007) To explore the potential resistance mechanisms, we have determined the spontaneous frequency-of-resistance against ULD1, ULD2 in *S. aureus*. Novobiocin, an antibiotic formerly used in clinical practice, has served as a reference compound. Novobiocin's main target is the DNA gyrase subunit B, but

second-step resistance mutations occasionally occur in Topoisomerase IV. (Fujimoto-Nakamura et al., 2005) This antibiotic is effective against certain Gram-positive infections, including those caused by *S. aureus*. (Bisacchi & Manchester, 2015; Walsh et al., 1985)

Using a standard protocol for spontaneous frequency-of-resistance analysis (Bell & MacLean, 2018; Ling et al., 2015), we have exposed 10^{10} to 10^{12} bacterial cells derived from stationary-phase cultures of *S. aureus* ATCC 700699 (VISA) and *S. aureus* ATCC 43300 (MRSA) to increasing concentrations of ULD1, ULD2, and novobiocin, respectively. We have assessed the frequency-of-resistance and the mutant prevention concentration (MPC) for all 3 compounds. MPC is the drug concentration threshold above which the proliferation of resistant mutants does not occur (i.e., the concentration required to avoid the emergence of all first-step resistant mutants). (Bell & MacLean, 2018) In agreement with prior laboratory studies and clinical observations, the frequency-of-resistance against novobiocin was relatively high (Fig 5), and an up-to 120-fold increment in the MIC of novobiocin in the isolated *S. aureus* mutants have been detected. (Fujimoto-Nakamura et al., 2005; Vickers et al., 2007) By sharp contrast, no resistant variants of *S. aureus* have been detected when the bacterial cells were exposed to ULD1 at concentrations 8-fold the wild-type MIC (Fig 5). Moreover, resistant mutants isolated upon exposure to ULD1 at lower compound concentrations provided only minor changes in ULD1 susceptibility.

To investigate the molecular basis of mild ULD1 resistance, we have collected 400 independently isolated, ULD1 resistant clones from the frequency-of-resistance assay plates and have sequenced their gyrB and parE genomic regions using Pacific Biosciences single-molecule real-time (SMRT) amplicon sequencing. Sequence analyses have revealed that all ULD1-resistant isolates had missense mutations that mapped to gyrB. Four different positions in the ULD1-binding pocket of GyrB (R144, G85, I175, T173) have mutated repeatedly. All the mutated amino acid residues in *S. aureus* are located in the binding pocket of GyrB and form secondary interactions with ULD1.

As ULD2 has a high affinity towards both of its target proteins and exerts an excellent dual-target enzyme inhibition, we hypothesized that the frequency-of-resistance against ULD2 could be exceptionally low. Notably, no ULD2 resistant mutants have emerged when 4×10^{12} *S. aureus* ATCC 700699 (VISA) cells were exposed to ULD2 at a concentration of only 4 times the wild-

type MIC (Fig 5). We estimate that the MPC is as low as 0.16 μg/mL for ULD1 and 0.08 μg/mL for ULD2 in *S. aureus* ATCC 700699 (VISA).

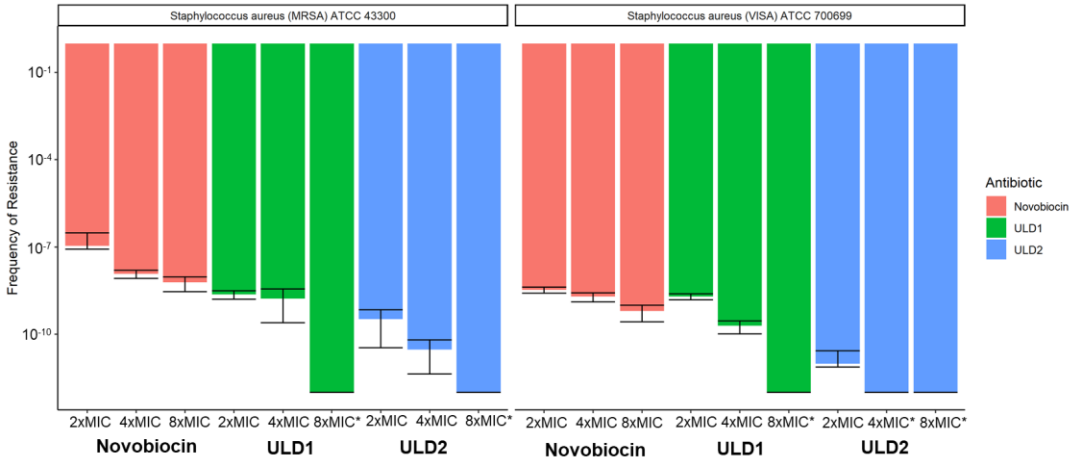

Figure 5. Spontaneous frequency-of-resistance of ULD1 and ULD2. Spontaneous frequency-of-resistance of ULD1, ULD2, and novobiocin in *S. aureus* MRSA ATCC 43300 (left panel) *S. aureus* VISA ATCC 700699 (right panel). Data are based on 10 independent biological replicates. Error bars indicate the 95% confidence interval. Asterisk (*) marks cases where the frequency-of-resistance was below 1×10^{-12}.

While these results were encouraging, our prior experience with gepotidacin suggests that combination of multiple, specific mutations at all drug targets, in the long run, can eventually render even multi-targeting antibiotics ineffective. (Szili et al., 2019) To test this possibility, we have repeated the frequency-of-resistance assays with 2 ULD1-resistant *S. aureus* VISA laboratory isolates, both of which carried a single mutation at GyrB, the primary target of ULD1/ULD2. These mutations—GyrB R144I and I175T—were relatively frequent in the isolated single-step resistant mutants, and they conferred a moderately decreased susceptibility to ULD1. Populations of these single-mutant strains have been exposed to increasing concentrations of ULD1 and ULD2, separately. Spontaneous resistant mutants have appeared at a frequency of 10^{-8}–10^{-11}. All isolated second-step resistant mutants have displayed a relatively low resistance level, i.e., they could be inhibited by 1 μg/mL of ULD2. Sequence analyses have revealed that all detected second-step mutations are localized at ParE, the other target of ULD1/ULD2, at positions that are homologous to the binding sites in GyrB (Table 3). In sum, the observed mutations provide strong evidence in support of a dual-targeting mechanism of action for ULD1 and ULD2.

Selection	GyrB	ParE	ULD1	ULD2
	Mutation		MIC (μg/mL)	
ULD1 at 16× MIC	R144I	F95Y	2	0.125
	R144I	R136L	1	0.125
	R144I	A120D	2	0.25
	R144I	R136G	2	0.25
ULD1 at 16× MIC	I175T	F95Y	4	0.25
	I175T	T166A	2	0.125
	I175T	R136G	4	0.5
	I175T	A120D	4	0.25
	I175T	T166I	2	0.25
ULD2 at 12× MIC	R144I	R136G	4	0.25
	R144I	A120D	2	0.125
	R144I	F95Y	2	0.25
ULD2 at 8× MIC	I175T	A120D	4	1

Table 3. Resistance level of second-step spontaneous ULD1- and ULD2-resistant mutants in *S. aureus* ATCC 700699. MICs were determined in MHBII medium at 37 °C by broth microdilution assay according to CLSI guidelines.

4.6. Evolution of resistance under long-term antibiotic exposure

We have also investigated whether long-term exposure to ULD1 and ULD2 could select for a high level of resistance. To this aim, we performed adaptive laboratory evolution experiments with VISA under ULD1, ULD2, and novobiocin stresses. We have employed a previously established protocol that aims to maximize the level of drug resistance in the evolving bacterial populations. (Sommer et al., 2017; Szili et al., 2019) To accurately assess potential resistance mechanisms, 10 parallel evolving populations have been exposed to gradually increasing concentrations of each compound. Following laboratory evolution, a single clone from each population has been isolated and subjected to drug susceptibility tests. In agreement with prior clinical observations and laboratory studies (Bisacchi & Manchester, 2015; Vickers et al., 2007), a high level of novobiocin-resistance has emerged rapidly (Fig 6A). In novobiocin-adapted strains, an up-to-320-fold increase in novobiocin MIC (i.e., 16 μg/mL) has been detected, compared with the wild type strain. In contrast, only a relatively modest, 25-fold increase in the MICs of ULD1

and ULD2 have been detected in lineages adapted to ULD1 or ULD2, respectively (1 μg/mL for ULD1 and 0.5 μg/mL for ULD2). In order to elucidate the molecular mechanisms underlying ULD2 resistance, 5 ULD2-adapted strains have been subjected to whole-genome sequencing. We have focused on de novo mutations that have accumulated in several lineages independently during the course of laboratory evolution. Such mutations have been found in the target proteins (GyrB, ParE), as well as in a regulator of purine biosynthesis (PurR), and another enzyme involved in the uridine diphosphate (UDP) biosynthesis pathway (PyrH). The exact roles of these mutations in shaping ULD1/ULD2 susceptibilities remain to be discovered.

Antibiotic resistance mutations frequently impact bacterial viability, and the associated fitness costs determine the spread and long-term maintenance of resistant populations in clinical settings. (Hughes & Andersson, 2015; Martínez et al., 2011) To explore the potential costs of resistance, we have investigated the growth phenotype of laboratory evolved, ULD1/ULD2 resistance-conferring *S. aureus* VISA isolates. Fitness was estimated by measuring the optical density at 600 nm (OD_{600}) of the population during 48 hours of growth in an antibiotic-free medium. ULD1/ULD2 resistant clones displayed a statistically significant decrease in growth compared to the wild type strain (Fig 6B) and formed tiny, slow-growing colonies on agar plates (Fig 6C). These data indicate that long-term exposure to ULD1 and ULD2 yields mutants with limited resistance and high associated fitness costs in an antibiotic-free environment.

Based on our prior experience regarding the link between gepotidacin and ciprofloxacin resistance, it was rational to hypothesize that novobiocin-resistant clinical isolates might interfere with the antibacterial effects of ULD1 and ULD2. To investigate potential cross-resistance, the MIC of ULD1 and ULD2 have been tested against 9 independently evolved novobiocin-resistant isolates. These strains have been found to display no cross-resistance to ULD2, and only a modest, up to 6-fold decrease in ULD1 susceptibility has been detected compared with the corresponding wild type strain (Fig 6D).

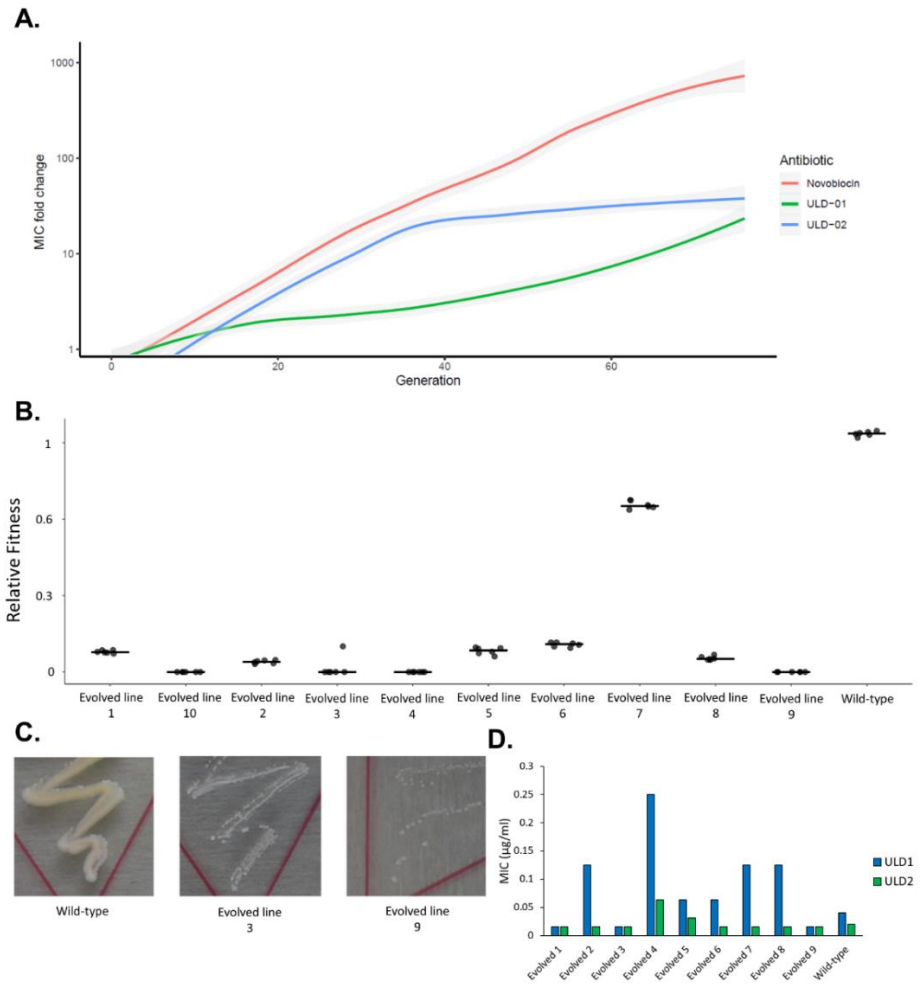

Figure 6. Adaptive laboratory evolution of *S. aureus* (VISA) ATCC 700699 to ULD1, ULD2, and novobiocin stresses. A. The figure displays increment in MIC level relative to wild type as a function of cell generation number. Data show the mean MIC fold-change based on 10, independently evolving populations. Gray area represents a 95% confidence interval. B. and C. Relative fitness (B) and growth phenotype (C) of ULD1-evolved and wild-type *S. aureus* VISA ATCC 700699. Fitness was approximated from the growth curves of isogenic microbial populations (see Materials and methods) and depicted as relative fitness compared with that of the wild type. Measurements were performed in 6 replicates. Growth phenotypes were observed in BHI agar plates and documented after 24 hours of incubation at 37 °C. D. Susceptibility of novobiocin-resistant *S. aureus* VISA ATCC 700699 mutants to ULD1 and ULD2. MICs were determined in MHBII medium at 37 °C by broth microdilution assay according to CLSI guidelines.

One of the independently evolved novobiocin-adapted strains displayed exceedingly slow growth, and therefore, it was omitted from the analysis.

4.7. *In vivo* efficacy of ULD1 and ULD2

Based on the potent antibacterial activities of ULD1 and ULD2, we have finally tested their *in vivo* efficacy in mice models of *S. aureus* infections. First, a murine model of human staphylococcal SSTI has been utilized. This preclinical model is extensively used to characterize the pharmacokinetic and pharmacodynamic properties of antistaphylococcal agents, as well as to predict their human clinical efficacy. (Kugelberg et al., 2005; Ling et al., 2015; Vingsbo Lundberg & Frimodt-Møller, 2013) Topical ULD1 and ULD2 treatments (in the form of ointments) were tested against *S. aureus* USA300 MRSA (BAA1556) and VISA and VRSA clinical isolates. USA300 MRSA clinical isolates are responsible for most community epidemics in the USA and are spreading worldwide. (Turner et al., 2019) Also, these 3 strains together are resistant to at least 9 distinct classes of antibiotics, including mupirocin, a last-resort antibiotic against SSTIs caused by multidrug-resistant *S. aureus*. Topical application of ULD1 and ULD2 has exerted a potent antibacterial activity (Fig 7A and 7B), comparable to that of mupirocin. Subsequent pharmacokinetic (PK) analyses indicate efficient skin penetration for both drugs, reaching a concentration of up to 300-times the MIC of ULD1 and ULD2 in wild-type *S. aureus* VISA.

We have also tested ULD1 in a neutropenic model of murine thigh infection. Intravenous (IV) administration of the drug resulted in potent antibacterial activity against *S. aureus* VISA infection (Fig 7C). Notably, the antibacterial activity of ULD1 was comparable to that of linezolid, a widely used clinical agent against systemic MRSA infections. (Watkins et al., 2012) Taken together, these *in vivo* efficacy data indicate that the ULD molecules could serve as a basis for successful future drug development efforts against both topical and systemic *S. aureus* infections.

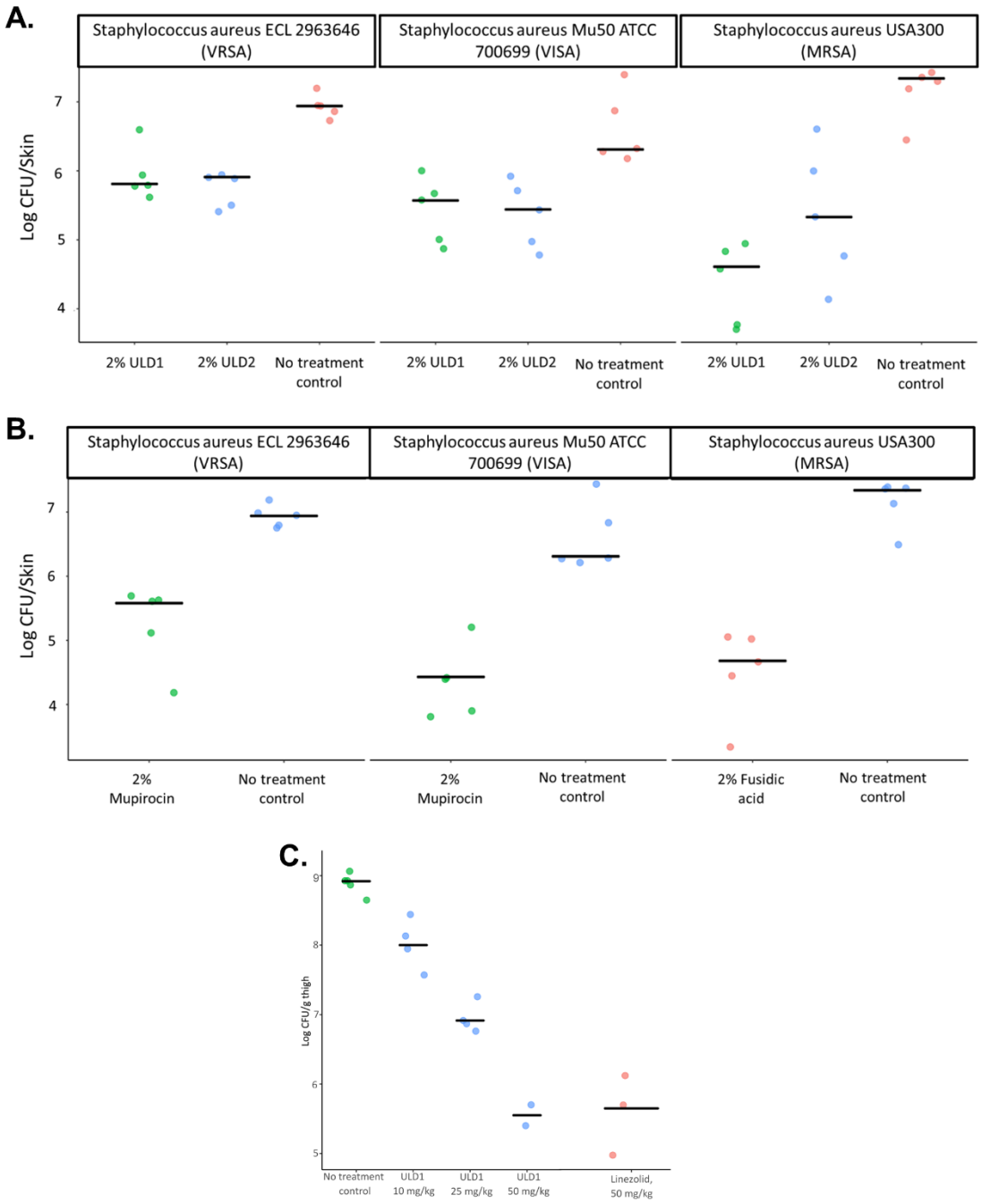

Figure 7. *In vivo* efficacy of ULD1 and ULD2 in 2 mouse infection models of *Staphylococcus aureus*. A. and B. *In vivo* efficacy of ULD1 and ULD2 in a mouse model of skin infection. Figure shows the number of CFUs after twice-daily topical antibiotic treatment (starting at 1 hour post infection). Three different *S. aureus* strains were used as inoculum in 5 immunocompetent mice per each group. Fig A and B displays results with ULD1, ULD2 (A) and positive control antibiotics fusidic acid and mupirocin (B), respectively. Skin tissue CFUs were

determined at 25 hours post infection. CFUs from each mouse are plotted as dots; the black line represents the average CFU in each experimental group. C. Efficacy of ULD1 in a neutropenic mouse infection of *S. aureus*. The figure shows the number of CFUs in response to antibiotic treatment, using linezolid as positive control. A standard neutropenic thigh infection model was employed with *S. aureus* VISA ATCC 700699 (for details, see Materials and methods). CFUs from thigh tissue homogenates were determined at 26 hours postinfection. The CFUs from each individual are plotted as dots, black line represents the average CFU in each experimental group.

5. Discussion

In this work, we mainly focused on resistance against multi-targeting antibiotics, by describing resistance development against DNA gyrase-topoisomerase inhibitors with notable dual-targeting activity.

Regarding gepotidacin we have demonstrated that two specific mutations in the genes encoding gepotidacin's targets can provide drastically elevated resistance. These two mutations (GyrA D82N and ParC D79N) show extreme synergism, together they confer an >2,000-fold resistance, while individually, they have only limited effects on susceptibility to gepotidacin. Alarmingly, the *K. pneumoniae* double mutant strain is as virulent as the wild type in a mouse infection model, suggesting that these mutations might have clinical significance. In line with these findings, *Neisseria gonorrhoeae* strains with reduced susceptibility to gepotidacin isolated in a human clinical phase 2b trial carried a ParC D86N mutation that is homologous to the ParC D79N mutation in *K. pneumoniae*. (Scangarella-Oman et al., 2018)

We have proposed that the quick resistance development is due what we termed the 'stepping stone' mechanism of acquiring resistance, when the prolonged clinical use of certain antibiotics can precondition bacterial populations to resistance development against novel antibiotics. In the case of gepotidacin, we demonstrated the possible connection between gepotidacin and fluoroquinolone antibiotics. Mutations linked to gepotidacin resistance (i.e., GyrA D82N and ParC D79N) increase resistance to ciprofloxacin and have been detected in clinical isolates of ciprofloxacin-resistant bacteria, including strains of *N. gonorrhoeae, Streptococcus, and Salmonella enterica*. Therefore, these isolates are expected to require only one extra mutational step to develop gepotidacin resistance.

ULD1 and ULD2 belong to a new class of dual-targeting antibacterial compounds that inhibit bacterial DNA gyrase and Topoisomerase IV protein complexes and are structurally distinct from novobiocin, gepotidacin, and fluoroquinolone antibiotics. They are potent inhibitors of the ATPase activities of GyrB and ParE and show a superior and balanced enzyme inhibition of both target proteins compared with novobiocin, an inhibitor of GyrB that has reached clinical practice but was later withdrawn. (Apothecon et al., 2009) ULD1 and ULD2 have broad-spectrum antibacterial activities against a wide range of pathogens, including multidrug-resistant clinical

isolates. The efficacy of ULD1 and ULD2 was tested against a broad panel of *S. aureus* clinical strains, including recently isolated MRSA and VISA variants. Approved drugs against staphylococcal infections fail to inhibit a significant fraction of these isolates, whereas both ULD1 and ULD2 are found to be potently active against all of them (MIC ≤ 1 μg/mL, see Fig 4). Using murine models of multidrug-resistant staphylococcal skin and thigh infections, ULD1 was shown to display potent efficacy both via topical and systemic administration.

ULD1 and ULD2 bypass existing and clinically widespread resistance mechanisms, including those that hinder the efficacy of other DNA gyrase and Topoisomerase IV inhibitors. Additionally, de novo resistance mutations against these compounds are rare and have a limited impact on resistance level. The MPC (i.e., the concentration required to prevent the emergence of single-step mutants) is exceptionally low for both compounds. Remarkably, all isolated double mutants have displayed low resistance level only, i.e., they could be inhibited by 1 μg/mL of ULD2. Thus, even combinations of specific resistance mutations provide only moderate changes in compound susceptibility. The adaptive laboratory evolution experiments further confirm that resistance by genomic mutations is exceedingly rare against ULD1/ULD2 and often come at a high fitness cost.

In summary, our work critically examined the concept of multi-targeting antibiotics in relation to yielding less resistance-prone antibiotics. We demonstrated that despite a balanced *in vivo* targeting of multiple proteins, resistance can rapidly emerge to antibiotics when the drug molecule's inhibitory effect depends merely on interactions with a few indispensable amino acids. Moreover, based on adaptive laboratory evolution and clinical data, we propose that target gene mutations conferring resistance to fluoroquinolones can facilitate resistance evolution to novel topoisomerase-targeting antimicrobials, including gepotidacin. This conclusion does not necessarily hold for the ULD molecules that have no related antibiotics in clinical rotation. Based on that multi-targeting might be a favorable approach if the antibiotic inhibits one or two completely novel targets, but scenarios like this should be examined in the future.

These findings might be relevant for other antibiotics currently in development. One example might be zoliflodacin (ETX0914), a novel bacterial topoisomerase inhibitor in human clinical trials. It shows promising activity against multidrug-resistant infections, including those caused by *N. gonorrhoeae*. (Basarab et al., 2015; Taylor, Marrazzo, et al., 2018) However, in this

species, mutations in GyrB have been reported to confer zoliflodacin resistance. One of these zoliflodacin-resistant mutants (D429N) has already been detected in clinical populations and naturally occurring zoliflodacin-resistant variants were also found to be highly resistant to fluoroquinolones. (Damião Gouveia et al., 2018; Foerster et al., 2015) Another relevant example outside the DNA gyrase – topoisomerase inhibitor family is SCH79797 and its derivative, Irresistin-16. SCH79797 is a repurposed drug that, according to recent data, shows antimicrobial activity with a unique mode of action, by simultaneously targeting folate metabolism and membrane integrity. In line with these findings, frequency of resistance against the drug in these first experiments was low and SCH79797 resistance did not develop while passaging the bacteria on sublethal concentration. (Martin et al., 2020) However, based on our experiences, these data worth revisiting in different bacterial species or with different methodologies.

6. References

Jim O'Neill: Tackling Drug-Resistant Infections Globally: Final Report and Recommendations (2016). Retrieved 6 January 2021, from https://amr-review.org/sites/default/files/160518_Final%20paper_with%20cover.pdf

Highlights of Prescribing Information - BAXDELA (delafloxacin) tablets, for oral use, BAXDELA (delafloxacin) for injection, for intravenous use (2017). Retrieved 7 January 2020, from https://www.accessdata.fda.gov/drugsatfda_docs/label/2017/208610s000,208611s000lbl.pdf

Altschul, S. F., Gish, W., Miller, W., Myers, E. W., & Lipman, D. J. (1990). Basic local alignment search tool. *Journal of Molecular Biology*, *215*(3), 403–410. https://doi.org/10.1016/S0022-2836(05)80360-2

Aminov, R. I. (2009). The role of antibiotics and antibiotic resistance in nature. *Environmental Microbiology*, *11*(12), 2970–2988. https://doi.org/10.1111/j.1462-2920.2009.01972.x

Antibiotic Hybrids: The Next Generation of Agents and Adjuvants against Gram-Negative Pathogens? | Clinical Microbiology Reviews. (n.d.). Retrieved 7 January 2021, from https://cmr.asm.org/content/31/2/e00077-17

Antibiotics Currently in Global Clinical Development. (n.d.). Retrieved 6 January 2021, from http://pew.org/1YkUFkT

Apothecon et al.; Withdrawal of Approval of 103 New Drug Applications and 35 Abbreviated New Drug Applications. (2009, February 11). Federal Register. https://www.federalregister.gov/documents/2009/02/11/E9-2901/apothecon-et-al-withdrawal-of-approval-of-103-new-drug-applications-and-35-abbreviated-new-drug

Årdal, C., Balasegaram, M., Laxminarayan, R., McAdams, D., Outterson, K., Rex, J. H., & Sumpradit, N. (2020). Antibiotic development—Economic, regulatory and societal challenges. *Nature Reviews Microbiology*, *18*(5), 267–274. https://doi.org/10.1038/s41579-019-0293-3

Basarab, G. S., Kern, G. H., McNulty, J., Mueller, J. P., Lawrence, K., Vishwanathan, K., Alm, R. A., Barvian, K., Doig, P., Galullo, V., Gardner, H., Gowravaram, M., Huband, M., Kimzey, A., Morningstar, M., Kutschke, A., Lahiri, S. D., Perros, M., Singh, R., … Newman, J. V. (2015). Responding to the challenge of untreatable gonorrhea: ETX0914, a first-in-class agent with a distinct mechanism-of-action against bacterial Type II topoisomerases. *Scientific Reports*, *5*(1), 11827. https://doi.org/10.1038/srep11827

Baym, M., Lieberman, T. D., Kelsic, E. D., Chait, R., Gross, R., Yelin, I., & Kishony, R. (2016). Spatiotemporal microbial evolution on antibiotic landscapes. *Science*, *353*(6304), 1147–1151. https://doi.org/10.1126/science.aag0822

Bell, G., & MacLean, C. (2018). The Search for 'Evolution-Proof' Antibiotics. *Trends in Microbiology*, *26*(6), 471–483. https://doi.org/10.1016/j.tim.2017.11.005

Biedenbach, D. J., Bouchillon, S. K., Hackel, M., Miller, L. A., Scangarella-Oman, N. E., Jakielaszek, C., & Sahm, D. F. (2016). In Vitro Activity of Gepotidacin, a Novel Triazaacenaphthylene Bacterial Topoisomerase Inhibitor, against a Broad Spectrum of Bacterial Pathogens. *Antimicrobial Agents and Chemotherapy*, *60*(3), 1918–1923. https://doi.org/10.1128/AAC.02820-15

Bisacchi, G. S., & Manchester, J. I. (2015). A New-Class Antibacterial—Almost. Lessons in Drug Discovery and Development: A Critical Analysis of More than 50 Years of Effort toward ATPase Inhibitors of DNA Gyrase and Topoisomerase IV. *ACS Infectious Diseases*, *1*(1), 4–41. https://doi.org/10.1021/id500013t

Bódi, Z., Farkas, Z., Nevozhay, D., Kalapis, D., Lázár, V., Csörgő, B., Nyerges, Á., Szamecz, B., Fekete, G., Papp, B., Araújo, H., Oliveira, J. L., Moura, G., Santos, M. A. S., Jr, T. S., Balázsi, G., & Pál, C. (2017). Phenotypic heterogeneity promotes adaptive evolution. *PLOS Biology*, *15*(5), e2000644. https://doi.org/10.1371/journal.pbio.2000644

Champoux, J. J. (2001). DNA Topoisomerases: Structure, Function, and Mechanism. *Annual Review of Biochemistry*, *70*(1), 369–413. https://doi.org/10.1146/annurev.biochem.70.1.369

Chen, F.-J., Lauderdale, T.-L., Ho, M., & Lo, H.-J. (2003). The Roles of Mutations in *gyrA*, *parC* , and *ompK35* in Fluoroquinolone Resistance in *Klebsiella pneumoniae*. *Microbial Drug Resistance*, *9*(3), 265–271. https://doi.org/10.1089/107662903322286472

Collin, F., Karkare, S., & Maxwell, A. (2011). Exploiting bacterial DNA gyrase as a drug target: Current state and perspectives. *Applied Microbiology and Biotechnology*, *92*(3), 479–497. https://doi.org/10.1007/s00253-011-3557-z

Confreres, A., & Maxwell, A. (1992). GyrB mutations which confer coumarin resistance also affect DNA supercoiling and ATP hydrolysis by Escherichia coli DNA gyrase. *Molecular Microbiology*, *6*(12), 1617–1624. https://doi.org/10.1111/j.1365-2958.1992.tb00886.x

Correia, S., Poeta, P., Hébraud, M., Capelo, J. L., & Igrejas, G. (2017). Mechanisms of quinolone action and resistance: Where do we stand? *Journal of Medical Microbiology*, *66*(5), 551–559. https://doi.org/10.1099/jmm.0.000475

Damião Gouveia, A. C., Unemo, M., & Jensen, J. S. (2018). In vitro activity of zoliflodacin (ETX0914) against macrolide-resistant, fluoroquinolone-resistant and antimicrobial-susceptible Mycoplasma genitalium strains. *Journal of Antimicrobial Chemotherapy*, *73*(5), 1291–1294. https://doi.org/10.1093/jac/dky022

D'Costa, V. M., King, C. E., Kalan, L., Morar, M., Sung, W. W. L., Schwarz, C., Froese, D., Zazula, G., Calmels, F., Debruyne, R., Golding, G. B., Poinar, H. N., & Wright, G. D. (2011). Antibiotic resistance is ancient. *Nature*, *477*(7365), 457–461. https://doi.org/10.1038/nature10388

DeRyke, C. A., Banevicius, M. A., Fan, H. W., & Nicolau, D. P. (2007). Bactericidal Activities of Meropenem and Ertapenem against Extended-Spectrum-β-Lactamase-Producing Escherichia coli and Klebsiella pneumoniae in a Neutropenic Mouse Thigh Model. *Antimicrobial Agents and Chemotherapy*, *51*(4), 1481–1486. https://doi.org/10.1128/AAC.00752-06

Drlica, K., Hiasa, H., Kerns, R., Malik, M., & Zhao, A. M. and X. (2009, July 31). *Quinolones: Action and Resistance Updated*. Current Topics in Medicinal Chemistry. https://www.eurekaselect.com/85153/article

Dykhuizen, D. E. (1990). Experimental Studies of Natural Selection in Bacteria. *Annual Review of Ecology and Systematics*, *21*(1), 373–398. https://doi.org/10.1146/annurev.es.21.110190.002105

Emmerson, A. M., & Jones, A. M. (2003). The quinolones: Decades of development and use. *Journal of Antimicrobial Chemotherapy*, *51*(suppl_1), 13–20. https://doi.org/10.1093/jac/dkg208

Farrell, D. J., Sader, H. S., Rhomberg, P. R., Scangarella-Oman, N. E., & Flamm, R. K. (2017). In Vitro Activity of Gepotidacin (GSK2140944) against Neisseria gonorrhoeae. *Antimicrobial Agents and Chemotherapy*, *61*(3). https://doi.org/10.1128/AAC.02047-16

Flamm, R. K., Farrell, D. J., Rhomberg, P. R., Scangarella-Oman, N. E., & Sader, H. S. (2017). Gepotidacin (GSK2140944) In Vitro Activity against Gram-Positive and Gram-Negative Bacteria. *Antimicrobial Agents and Chemotherapy*, *61*(7). https://doi.org/10.1128/AAC.00468-17

Foerster, S., Golparian, D., Jacobsson, S., Hathaway, L. J., Low, N., Shafer, W. M., Althaus, C. L., & Unemo, M. (2015). Genetic Resistance Determinants, In Vitro Time-Kill Curve Analysis and Pharmacodynamic Functions for the Novel Topoisomerase II Inhibitor ETX0914 (AZD0914) in Neisseria gonorrhoeae. *Frontiers in Microbiology*, *6*. https://doi.org/10.3389/fmicb.2015.01377

Fujimoto-Nakamura, M., Ito, H., Oyamada, Y., Nishino, T., & Yamagishi, J. (2005). Accumulation of Mutations in both gyrB and parE Genes Is Associated with High-Level Resistance to Novobiocin in Staphylococcus aureus. *Antimicrobial Agents and Chemotherapy*, *49*(9), 3810–3815. https://doi.org/10.1128/AAC.49.9.3810-3815.2005

Garoff, L., Pietsch, F., Huseby, D. L., Lilja, T., Brandis, G., & Hughes, D. (2020). Population Bottlenecks Strongly Influence the Evolutionary Trajectory to Fluoroquinolone Resistance in Escherichia coli. *Molecular Biology and Evolution*, *37*(6), 1637–1646. https://doi.org/10.1093/molbev/msaa032

Gross, C. H., Parsons, J. D., Grossman, T. H., Charifson, P. S., Bellon, S., Jernee, J., Dwyer, M., Chambers, S. P., Markland, W., Botfield, M., & Raybuck, S. A. (2003). Active-Site Residues of Escherichia coli DNA Gyrase Required in Coupling ATP Hydrolysis to DNA Supercoiling and Amino Acid Substitutions Leading to Novobiocin Resistance. *Antimicrobial Agents and Chemotherapy*, *47*(3), 1037–1046. https://doi.org/10.1128/AAC.47.3.1037-1046.2003

Guide for the Care and Use of Laboratory Animals.pdf. (n.d.). Retrieved 8 March 2021, from https://grants.nih.gov/grants/olaw/guide-for-the-care-and-use-of-laboratory-animals.pdf

Hasenbrink, G., Schwarzer, S., Kolacna, L., Ludwig, J., Sychrova, H., & Lichtenberg-Fraté, H. (2005). Analysis of the mKir2.1 channel activity in potassium influx defective Saccharomyces cerevisiae strains determined as changes in growth characteristics. *FEBS Letters*, *579*(7), 1723–1731. https://doi.org/10.1016/j.febslet.2005.02.025

Heide, L. (2009). Genetic engineering of antibiotic biosynthesis for the generation of new aminocoumarins. *Biotechnology Advances*, *27*(6), 1006–1014. https://doi.org/10.1016/j.biotechadv.2009.05.017

Hermes, J. D., Parekh, S. M., Blacklow, S. C., Koster, H., & Knowles, J. R. (1989). A reliable method for random mutagenesis: The generation of mutant libraries using spiked oligodeoxyribonucleotide primers. *Gene*, *84*(1), 143–151. https://doi.org/10.1016/0378-1119(89)90148-0

Hooper, D. C., & Jacoby, G. A. (2015). Mechanisms of drug resistance: Quinolone resistance. *Annals of the New York Academy of Sciences*, *1354*(1), 12–31. https://doi.org/10.1111/nyas.12830

Hooper, D. C., & Jacoby, G. A. (2016). Topoisomerase Inhibitors: Fluoroquinolone Mechanisms of Action and Resistance. *Cold Spring Harbor Perspectives in Medicine*, *6*(9), a025320. https://doi.org/10.1101/cshperspect.a025320

Hughes, D., & Andersson, D. I. (2015). Evolutionary consequences of drug resistance: Shared principles across diverse targets and organisms. *Nature Reviews Genetics*, *16*(8), 459–471. https://doi.org/10.1038/nrg3922

Ince, D., Zhang, X., Silver, L. C., & Hooper, D. C. (2002). Dual Targeting of DNA Gyrase and Topoisomerase IV: Target Interactions of Garenoxacin (BMS-284756, T-3811ME), a New Desfluoroquinolone. *Antimicrobial Agents and Chemotherapy*, *46*(11), 3370–3380. https://doi.org/10.1128/AAC.46.11.3370-3380.2002

Jackson, N., Czaplewski, L., & Piddock, L. J. V. (2018). Discovery and development of new antibacterial drugs: Learning from experience? *Journal of Antimicrobial Chemotherapy*, *73*(6), 1452–1459. https://doi.org/10.1093/jac/dky019

Karcagi, I., Draskovits, G., Umenhoffer, K., Fekete, G., Kovács, K., Méhi, O., Balikó, G., Szappanos, B., Györfy, Z., Fehér, T., Bogos, B., Blattner, F. R., Pál, C., Pósfai, G., & Papp, B. (2016). Indispensability of Horizontally Transferred Genes and Its Impact on Bacterial Genome Streamlining. *Molecular Biology and Evolution*, *33*(5), 1257–1269. https://doi.org/10.1093/molbev/msw009

Klahn, P., & Brönstrup, M. (2017). Bifunctional antimicrobial conjugates and hybrid antimicrobials. *Natural Product Reports*, *34*(7), 832–885. https://doi.org/10.1039/C7NP00006E

Koboldt, D. C., Zhang, Q., Larson, D. E., Shen, D., McLellan, M. D., Lin, L., Miller, C. A., Mardis, E. R., Ding, L., & Wilson, R. K. (2012). VarScan 2: Somatic mutation and copy number alteration discovery in cancer by exome sequencing. *Genome Research*, *22*(3), 568–576. https://doi.org/10.1101/gr.129684.111

Krapp, F., Ozer, E. A., Qi, C., & Hauser, A. R. (2018). Case Report of an Extensively Drug-Resistant Klebsiella pneumoniae Infection With Genomic Characterization of the Strain and Review of Similar Cases in the United States. *Open Forum Infectious Diseases*, *5*(ofy074). https://doi.org/10.1093/ofid/ofy074

Kugelberg, E., Norström, T., Petersen, T. K., Duvold, T., Andersson, D. I., & Hughes, D. (2005). Establishment of a Superficial Skin Infection Model in Mice by Using Staphylococcus aureus and Streptococcus pyogenes. *Antimicrobial Agents and Chemotherapy*, *49*(8), 3435–3441. https://doi.org/10.1128/AAC.49.8.3435-3441.2005

Lázár, V., Martins, A., Spohn, R., Daruka, L., Grézal, G., Fekete, G., Számel, M., Jangir, P. K., Kintses, B., Csörgo, B., Nyerges, Á., Györkei, Á., Kincses, A., Dér, A., Walter, F. R., Deli, M. A., Urbán, E., Hegedus, Z., Olajos, G., … Pál, C. (2018). Antibiotic-resistant bacteria show widespread collateral sensitivity to antimicrobial peptides. *Nature Microbiology*, *3*(6), 718–731. https://doi.org/10.1038/s41564-018-0164-0

Li, H., & Durbin, R. (2009). Fast and accurate short read alignment with Burrows–Wheeler transform. *Bioinformatics*, *25*(14), 1754–1760. https://doi.org/10.1093/bioinformatics/btp324

Ling, L. L., Schneider, T., Peoples, A. J., Spoering, A. L., Engels, I., Conlon, B. P., Mueller, A., Schäberle, T. F., Hughes, D. E., Epstein, S., Jones, M., Lazarides, L., Steadman, V. A., Cohen, D. R., Felix, C. R., Fetterman, K. A., Millett, W. P., Nitti, A. G., Zullo, A. M., … Lewis, K. (2015). A new antibiotic kills pathogens without detectable resistance. *Nature*, *517*(7535), 455–459. https://doi.org/10.1038/nature14098

Martin, J. K., Sheehan, J. P., Bratton, B. P., Moore, G. M., Mateus, A., Li, S. H.-J., Kim, H., Rabinowitz, J. D., Typas, A., Savitski, M. M., Wilson, M. Z., & Gitai, Z. (2020). A Dual-Mechanism Antibiotic Kills Gram-Negative Bacteria and Avoids Drug Resistance. *Cell*, *181*(7), 1518-1532.e14. https://doi.org/10.1016/j.cell.2020.05.005

Martínez, J. L., Baquero, F., & Andersson, D. I. (2007). Predicting antibiotic resistance. *Nature Reviews Microbiology*, *5*(12), 958–965. https://doi.org/10.1038/nrmicro1796

Martínez, J. L., Baquero, F., & Andersson, D. I. (2011). Beyond serial passages: New methods for predicting the emergence of resistance to novel antibiotics. *Current Opinion in Pharmacology*, *11*(5), 439–445. https://doi.org/10.1016/j.coph.2011.07.005

Munck, C., Gumpert, H. K., Wallin, A. I. N., Wang, H. H., & Sommer, M. O. A. (2014). Prediction of resistance development against drug combinations by collateral responses to component drugs. *Science Translational Medicine*, *6*(262), 262ra156-262ra156. https://doi.org/10.1126/scitranslmed.3009940

Nöllmann, M., Crisona, N. J., & Arimondo, P. B. (2007). Thirty years of Escherichia coli DNA gyrase: From in vivo function to single-molecule mechanism. *Biochimie*, *89*(4), 490–499. https://doi.org/10.1016/j.biochi.2007.02.012

Nyerges, Á., Csörgő, B., Draskovits, G., Kintses, B., Szili, P., Ferenc, G., Révész, T., Ari, E., Nagy, I., Bálint, B., Vásárhelyi, B. M., Bihari, P., Számel, M., Balogh, D., Papp, H., Kalapis, D., Papp, B., & Pál, C. (2018). Directed evolution of multiple genomic loci allows the prediction of antibiotic resistance. *Proceedings of the National Academy of Sciences*, *115*(25), E5726–E5735. https://doi.org/10.1073/pnas.1801646115

Nyerges, Á., Csörgő, B., Nagy, I., Bálint, B., Bihari, P., Lázár, V., Apjok, G., Umenhoffer, K., Bogos, B., Pósfai, G., & Pál, C. (2016). A highly precise and portable genome engineering method allows comparison of mutational effects across bacterial species. *Proceedings of the National Academy of Sciences*, *113*(9), 2502–2507. https://doi.org/10.1073/pnas.1520040113

Nyerges, A., Tomašič, T., Durcik, M., Revesz, T., Szili, P., Draskovits, G., Bogar, F., Skok, Ž., Zidar, N., Ilaš, J., Zega, A., Kikelj, D., Daruka, L., Kintses, B., Vasarhelyi, B., Foldesi, I., Kata, D., Welin, M., Kimbung, R., … Pal, C. (2020). Rational design of balanced dual-targeting antibiotics with limited resistance. *PLOS Biology*, *18*(10), e3000819. https://doi.org/10.1371/journal.pbio.3000819

Oblak, M., & Solmajer, M. K. and T. (2007, July 31). *Discovery and Development of ATPase Inhibitors of DNA Gyrase as Antibacterial Agents*. Current Medicinal Chemistry. https://www.eurekaselect.com/59622/article

Oldfield, E., & Feng, X. (2014). Resistance-resistant antibiotics. *Trends in Pharmacological Sciences*, *35*(12), 664–674. https://doi.org/10.1016/j.tips.2014.10.007

O'Riordan, W., Tiffany, C., Scangarella-Oman, N., Perry, C., Hossain, M., Ashton, T., & Dumont, E. (2017). Efficacy, Safety, and Tolerability of Gepotidacin (GSK2140944) in the Treatment of Patients with Suspected or Confirmed Gram-Positive Acute Bacterial Skin and Skin Structure Infections. *Antimicrobial Agents and Chemotherapy*, *61*(6). https://doi.org/10.1128/AAC.02095-16

Payne, D., Gwynn, M., Holmes, D., & Pompliano, D. (2007). Drugs for Bad Bugs: Confronting the Challenges of Antibacterial Discovery. *Nature Reviews. Drug Discovery*, *6*, 29–40. https://doi.org/10.1038/nrd2201

Publications: Microbiology Today: Book Reviews. (n.d.). Retrieved 10 January 2021, from https://socgenmicrobiol.org.uk/pubs/micro_today/book_reviews/MTMAY04/MTM04_25.cfm

Quinlan, A. R., & Hall, I. M. (2010). BEDTools: A flexible suite of utilities for comparing genomic features. *Bioinformatics*, *26*(6), 841–842. https://doi.org/10.1093/bioinformatics/btq033

Ramakrishnan, K., Salinas, R. C., & Higuita, N. I. A. (2015). Skin and Soft Tissue Infections. *American Family Physician*, *92*(6), 474–483.

Ricaurte, D. E., Martínez-García, E., Nyerges, Á., Pál, C., Lorenzo, V. de, & Aparicio, T. (2018). A standardized workflow for surveying recombinases expands bacterial genome-editing capabilities. *Microbial Biotechnology*, *11*(1), 176–188. https://doi.org/10.1111/1751-7915.12846

Rossolini, G. M., Arena, F., Pecile, P., & Pollini, S. (2014). Update on the antibiotic resistance crisis. *Current Opinion in Pharmacology*, *18*, 56–60. https://doi.org/10.1016/j.coph.2014.09.006

Scangarella-Oman, N. E., Hossain, M., Dixon, P. B., Ingraham, K., Min, S., Tiffany, C. A., Perry, C. R., Raychaudhuri, A., Dumont, E. F., Huang, J., Hook, E. W., & Miller, L. A. (2018). Microbiological Analysis from a Phase 2 Randomized Study in Adults Evaluating Single Oral Doses of Gepotidacin in the Treatment of Uncomplicated Urogenital Gonorrhea Caused by Neisseria gonorrhoeae. *Antimicrobial Agents and Chemotherapy*, *62*(12). https://doi.org/10.1128/AAC.01221-18

Scangarella-Oman, N. E., Ingraham, K. A., Tiffany, C. A., Tomsho, L., Horn, S. F. V., Mayhew, D. N., Perry, C. R., Ashton, T. C., Dumont, E. F., Huang, J., Brown, J. R., & Miller, L. A. (2020). In Vitro Activity and Microbiological Efficacy of Gepotidacin from a Phase 2, Randomized, Multicenter, Dose-Ranging Study in Patients with Acute Bacterial Skin and Skin Structure Infections. *Antimicrobial Agents and Chemotherapy*, *64*(3). https://doi.org/10.1128/AAC.01302-19

Silver, L. L. (2007). Multi-targeting by monotherapeutic antibacterials. *Nature Reviews Drug Discovery*, *6*(1), 41–55. https://doi.org/10.1038/nrd2202

Sommer, M. O. A., Munck, C., Toft-Kehler, R. V., & Andersson, D. I. (2017). Prediction of antibiotic resistance: Time for a new preclinical paradigm? *Nature Reviews Microbiology*, *15*(11), 689–696. https://doi.org/10.1038/nrmicro.2017.75

Spellberg, B., Powers, J. H., Brass, E. P., Miller, L. G., & Edwards, J. E., Jr. (2004). Trends in Antimicrobial Drug Development: Implications for the Future. *Clinical Infectious Diseases*, *38*(9), 1279–1286. https://doi.org/10.1086/420937

Strahilevitz, J., & Hooper, D. C. (2005). Dual Targeting of Topoisomerase IV and Gyrase To Reduce Mutant Selection: Direct Testing of the Paradigm by Using WCK-1734, a New Fluoroquinolone, and Ciprofloxacin. *Antimicrobial Agents and Chemotherapy*, *49*(5), 1949–1956. https://doi.org/10.1128/AAC.49.5.1949-1956.2005

Sugino, A., Higgins, N. P., Brown, P. O., Peebles, C. L., & Cozzarelli, N. R. (1978). Energy coupling in DNA gyrase and the mechanism of action of novobiocin. *Proceedings of the National Academy of Sciences*, *75*(10), 4838–4842. https://doi.org/10.1073/pnas.75.10.4838

Suzuki, S., Horinouchi, T., & Furusawa, C. (2015). Suppression of antibiotic resistance acquisition by combined use of antibiotics. *Journal of Bioscience and Bioengineering*, *120*(4), 467–469. https://doi.org/10.1016/j.jbiosc.2015.02.003

Szili, P., Draskovits, G., Révész, T., Bogár, F., Balogh, D., Martinek, T., Daruka, L., Spohn, R., Vásárhelyi, B. M., Czikkely, M., Kintses, B., Grézal, G., Ferenc, G., Pál, C., & Nyerges, Á. (2019). Rapid Evolution of Reduced Susceptibility against a Balanced Dual-Targeting Antibiotic through Stepping-Stone Mutations. *Antimicrobial Agents and Chemotherapy*, *63*(9). https://doi.org/10.1128/AAC.00207-19

Tamma, P. D., Cosgrove, S. E., & Maragakis, L. L. (2012). Combination Therapy for Treatment of Infections with Gram-Negative Bacteria. *Clinical Microbiology Reviews*, *25*(3), 450–470. https://doi.org/10.1128/CMR.05041-11

Tan, C. M., Therien, A. G., Lu, J., Lee, S. H., Caron, A., Gill, C. J., Lebeau-Jacob, C., Benton-Perdomo, L., Monteiro, J. M., Pereira, P. M., Elsen, N. L., Wu, J., Deschamps, K., Petcu, M., Wong, S., Daigneault, E., Kramer, S., Liang, L., Maxwell, E., … Roemer, T. (2012). Restoring Methicillin-Resistant Staphylococcus aureus Susceptibility to β-Lactam Antibiotics. *Science Translational Medicine*, *4*(126), 126ra35-126ra35. https://doi.org/10.1126/scitranslmed.3003592

Tari, L. W., Li, X., Trzoss, M., Bensen, D. C., Chen, Z., Lam, T., Zhang, J., Lee, S. J., Hough, G., Phillipson, D., Akers-Rodriguez, S., Cunningham, M. L., Kwan, B. P., Nelson, K. J., Castellano, A., Locke, J. B., Brown-Driver, V., Murphy, T. M., Ong, V. S., … Finn, J. (2013). Tricyclic GyrB/ParE (TriBE) inhibitors: A new class of broad-spectrum dual-targeting antibacterial agents. *PloS One*, *8*(12), e84409. https://doi.org/10.1371/journal.pone.0084409

Taylor, S. N., Marrazzo, J., Batteiger, B. E., Edward W. Hook, I. I. I., Seña, A. C., Long, J., Wierzbicki, M. R., Kwak, H., Johnson, S. M., Lawrence, K., & Mueller, J. (2018). Single-Dose Zoliflodacin (ETX0914) for Treatment of Urogenital Gonorrhea. *New England Journal of Medicine*. https://doi.org/10.1056/NEJMoa1706988

Taylor, S. N., Morris, D. H., Avery, A. K., Workowski, K. A., Batteiger, B. E., Tiffany, C. A., Perry, C. R., Raychaudhuri, A., Scangarella-Oman, N. E., Hossain, M., & Dumont, E. F. (2018). Gepotidacin for the Treatment of Uncomplicated Urogenital Gonorrhea: A Phase 2, Randomized, Dose-Ranging, Single-Oral Dose Evaluation. *Clinical Infectious Diseases*, *67*(4), 504–512. https://doi.org/10.1093/cid/ciy145

Tillotson, G. (2018). A crucial list of pathogens. *The Lancet Infectious Diseases*, *18*(3), 234–236. https://doi.org/10.1016/S1473-3099(17)30754-5

Tomašič, T., Katsamakas, S., Hodnik, Ž., Ilaš, J., Brvar, M., Solmajer, T., Montalvão, S., Tammela, P., Banjanac, M., Ergović, G., Anderluh, M., Mašič, L. P., & Kikelj, D. (2015). Discovery of 4,5,6,7-Tetrahydrobenzo[1,2-d]thiazoles as Novel DNA Gyrase Inhibitors Targeting the ATP-Binding Site. *Journal of Medicinal Chemistry*, *58*(14), 5501–5521. https://doi.org/10.1021/acs.jmedchem.5b00489

Turner, N. A., Sharma-Kuinkel, B. K., Maskarinec, S. A., Eichenberger, E. M., Shah, P. P., Carugati, M., Holland, T. L., & Fowler, V. G. (2019). Methicillin-resistant Staphylococcus aureus: An overview of basic and clinical research. *Nature Reviews Microbiology*, *17*(4), 203–218. https://doi.org/10.1038/s41579-018-0147-4

V_9.0_Breakpoint_Tables.pdf. (n.d.). Retrieved 6 March 2021, from https://eucast.org/fileadmin/src/media/PDFs/EUCAST_files/Breakpoint_tables/v_9.0_Breakpoint_Tables.pdf

Velkov, T., Bergen, P. J., Lora-Tamayo, J., Landersdorfer, C. B., & Li, J. (2013). PK/PD models in antibacterial development. *Current Opinion in Microbiology*, *16*(5), 573–579. https://doi.org/10.1016/j.mib.2013.06.010

Vickers, A. A., O'Neill, A. J., & Chopra, I. (2007). Emergence and maintenance of resistance to fluoroquinolones and coumarins in Staphylococcus aureus: Predictions from in vitro studies. *Journal of Antimicrobial Chemotherapy*, *60*(2), 269–273. https://doi.org/10.1093/jac/dkm191

Vingsbo Lundberg, C., & Frimodt-Møller, N. (2013). Efficacy of topical and systemic antibiotic treatment of meticillin-resistant Staphylococcus aureus in a murine superficial skin wound infection model. *International Journal of Antimicrobial Agents*, *42*(3), 272–275. https://doi.org/10.1016/j.ijantimicag.2013.05.008

Walsh, T. J., Hansen, S. L., Tatem, B. A., Auger, F., & Standiford, H. C. (1985). Activity of novobiocin against methicillin-resistantStaphylococcusaureus. *Journal of Antimicrobial Chemotherapy*, *15*(4), 435–440. https://doi.org/10.1093/jac/15.4.435

Wang, H. H., & Church, G. M. (2011). Chapter eighteen - Multiplexed Genome Engineering and Genotyping Methods: Applications for Synthetic Biology and Metabolic Engineering. In C. Voigt (Ed.), *Methods in Enzymology* (Vol. 498, pp. 409–426). Academic Press. https://doi.org/10.1016/B978-0-12-385120-8.00018-8

Wang, H. H., Xu, G., Vonner, A. J., & Church, G. (2011). Modified bases enable high-efficiency oligonucleotide-mediated allelic replacement via mismatch repair evasion. *Nucleic Acids Research*, *39*(16), 7336–7347. https://doi.org/10.1093/nar/gkr183

Warringer, J., & Blomberg, A. (2003). Automated screening in environmental arrays allows analysis of quantitative phenotypic profiles in Saccharomyces cerevisiae. *Yeast*, *20*(1), 53–67. https://doi.org/10.1002/yea.931

Watkins, R. R., Lemonovich, T. L., & File, T. M. (2012). An evidence-based review of linezolid for the treatment of methicillin-resistant Staphylococcus aureus (MRSA): Place in therapy. *Core Evidence*, *7*, 131–143. https://doi.org/10.2147/CE.S33430

Wohlkonig, A., Chan, P. F., Fosberry, A. P., Homes, P., Huang, J., Kranz, M., Leydon, V. R., Miles, T. J., Pearson, N. D., Perera, R. L., Shillings, A. J., Gwynn, M. N., & Bax, B. D. (2010). Structural basis of quinolone inhibition of type IIA topoisomerases and target-mediated resistance. *Nature Structural & Molecular Biology*, *17*(9), 1152–1153. https://doi.org/10.1038/nsmb.1892

Yoshida, H., Bogaki, M., Nakamura, M., & Nakamura, S. (1990). Quinolone resistance-determining region in the DNA gyrase gyrA gene of Escherichia coli. *Antimicrobial Agents and Chemotherapy*, *34*(6), 1271–1272. https://doi.org/10.1128/AAC.34.6.1271

Yoshida, H., Bogaki, M., Nakamura, M., Yamanaka, L. M., & Nakamura, S. (1991). Quinolone resistance-determining region in the DNA gyrase gyrB gene of Escherichia coli. *Antimicrobial Agents and Chemotherapy*, *35*(8), 1647–1650. https://doi.org/10.1128/AAC.35.8.1647